Electronic Supplementary Information for:

Tetrad or triad? Insights from a versatile Fe(II) structural and functional model of the 3-his 1-carboxylate tetrad in C-C bond cleaving dioxygenase enzymes

Adam Fadul;[a] Thomas Cundari [b] Jeffery Bertke;[c] Santiago A. Toledo [a]

a. Department of Chemistry, American University, 4400 Massachusetts Ave NW, Washington, DC, 20016, United States of America.
b. Department of Chemistry, University of North Texas, 1155 Union Cir, Denton, Texas 76203, United States of America.
c. Department of Chemistry, Georgetown University, 3700 O St NW, Washington, DC, 20057, United States of America.

Characterization of complex 1

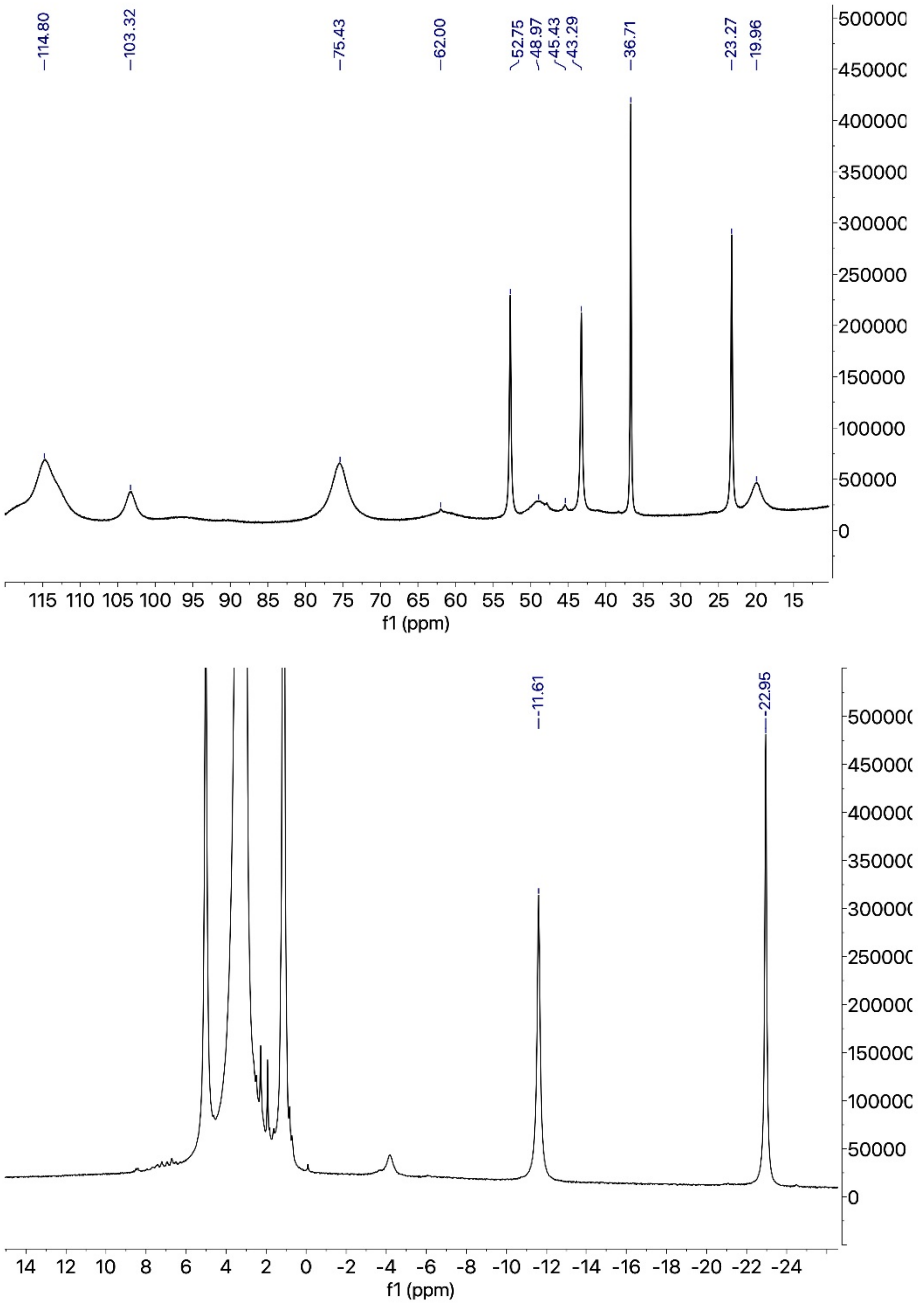

Figure S1: Paramagnetic ^{1}H-NMR of **1** in CD_3OD under anaerobic conditions.

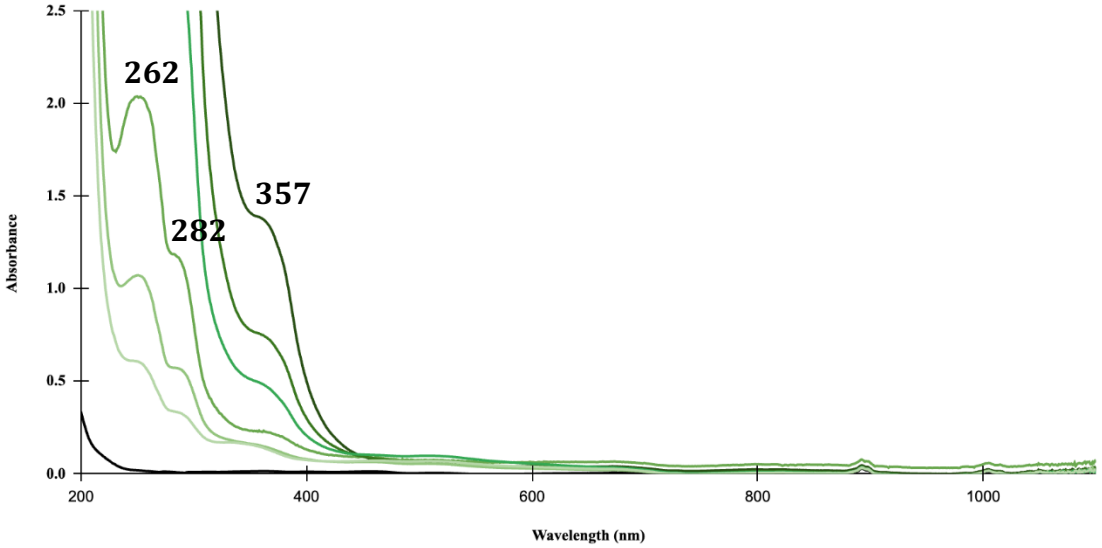

Figure S2: Quantitative UV-Visible spectrum of **1** in MeCN. Characteristic absorption shoulders are apparent at 357 nm and 282 nm. An absorption peak is also observed at 262 nm. The following molar extinction coefficients were obtained: ε_{357}= 641 $M^{-1}cm^{-1}$, ε_{282}= 5740 $M^{-1}cm^{-1}$, and ε_{262}= 9360 $M^{-1}cm^{-1}$.

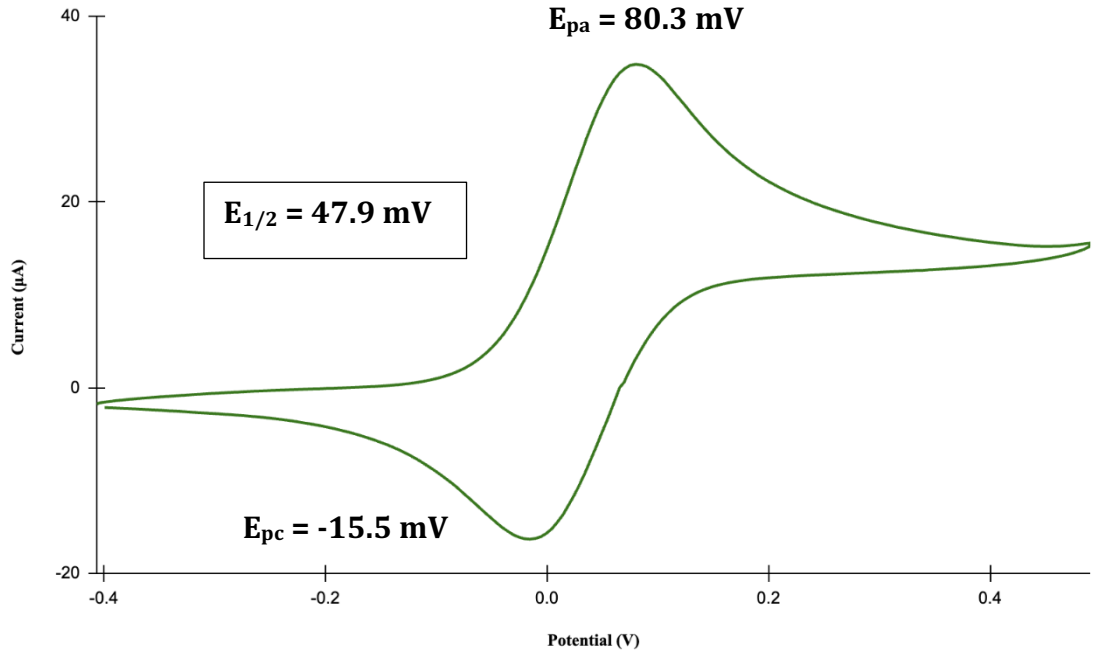

Figure S3: Cyclic voltammogram for complex **1** in MeCN (1.5mM) containing $[NBu_4][PF_6]$ (0.1M) as the supporting electrolyte. Scan rate 250 mV/sec. Potentials reported vs. Fc/Fc^+.

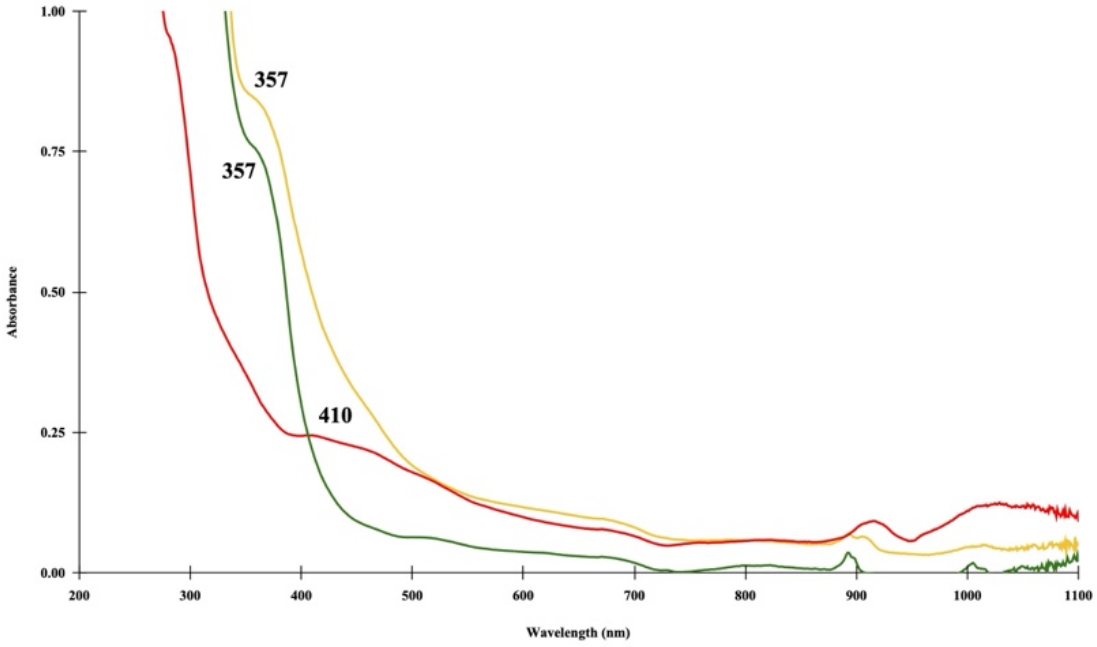

Figure S4: UV-vis spectrum of **1** under anaerobic conditions in MeCN, Acetone, and MeOH (green, yellow, and red traces respectively).

Atlantic Microlab, Inc.

6180 Atlantic Blvd. Suite M
Norcross, GA 30071
www.atlanticmicrolab.com

Sample No. Fe N3O SAT

Professor/Supervisor: Santiago Toledo

PO# / CC#

Company/School American University
Dept. Chemistry
Address 4400 Massachusetts Ave NW
City, State, Zip Washington DC, 20016
Name Santiago Toledo Date 09/23/25
Phone 2028857496

Element	Theory	Found	
C	47.29	46.89	
H	5.68	5.36	
N	7.88	7.34	

Single ☒ Duplicate ☐
Elements Present: Fe, C, N, H, S, O, F
Analyze for: C, H, N
Hygroscopic ☒ Explosive ☐
M.P. ____ B.P. ____
To be dried: Yes ☐ No ☒
Temp. ____ Vac. ____ Time ____
Rush Service ☐ Rush service guarantees analyses will be completed and results available by 5 PM EST on the day the sample is received by 11 AM.
Include Email Address or FAX # Below

Date Received SEP 24 2025 Date Completed SEP 25 2025
Remarks: Very air (O_2) sensitive + Moisture sensitive MW 533.38 g/mol

Image S1: Elemental analysis results for **1** (C, H, N only).

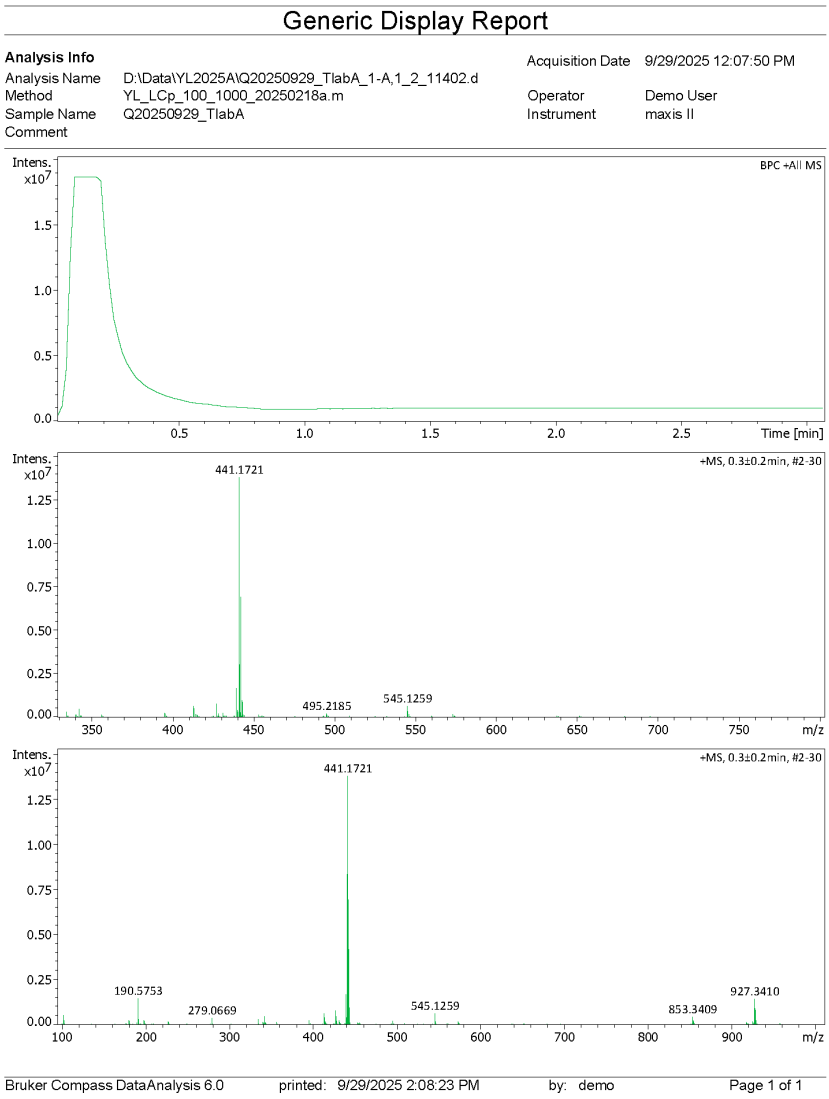

Image S2: ESI-MS of **1.** The calculated mass for 1 is 545.3 g/mol. The pentacoordinate complex **1** without the bound triflate counterion is 396.3 g/mol. The most prominent peak in the ESI above shows a peak at 441.1721 m/z and a minor peak at 545.1259 m/z. The first one corresponds to the addition of a mass of 45 mass units, which we attribute to the binding of formate (45 g/mol) to a ferric version of complex **1**. This formulation will give the complex a charge of +1, showing the observed m/z. This apparent oxidation would be expected given the sensitivity of **1** to reacting with O_2. Similarly, the m/z at 545 indicates a ferric triflate-bound complex, which would have a charge of +1. The presence of formate is not unusual in the spectrometer that is normally connected to an LC instrument.

Biomimetic oxidative C-C bond cleaving reactivity and general oxidative reactivity controls

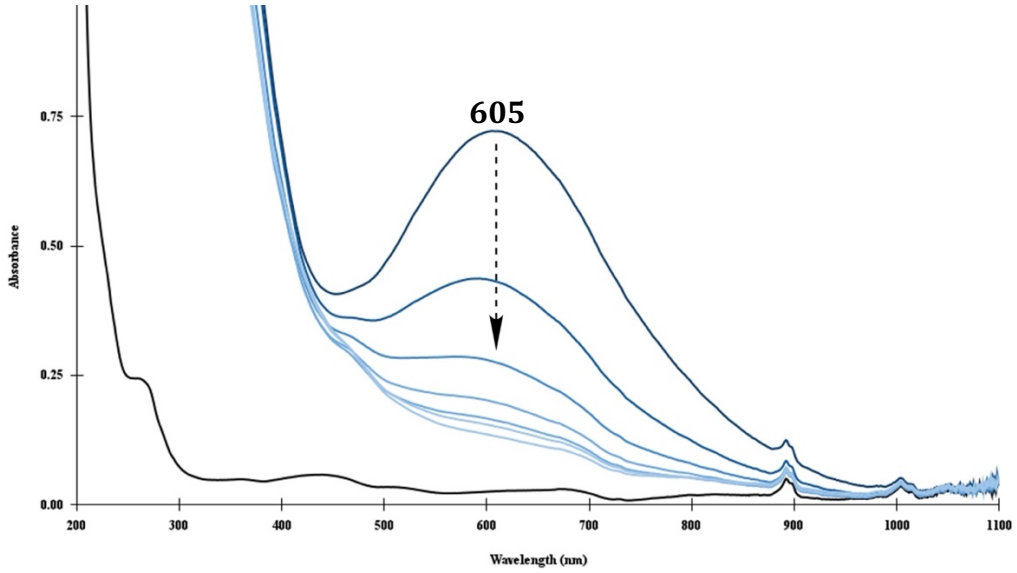

Figure S5: Time-lapse UV-Visible spectrum showing monitoring the 605 nm band of the dioxygenation C-C cleavage reaction of 3DHPD mediated by **1** in MeCN at room temperature. UV-Visible traces were recorded 3, 4.5, 6.5, 8, 9.5, 11, and 14 hours post oxygenation (blue traces of decreasing darkness).

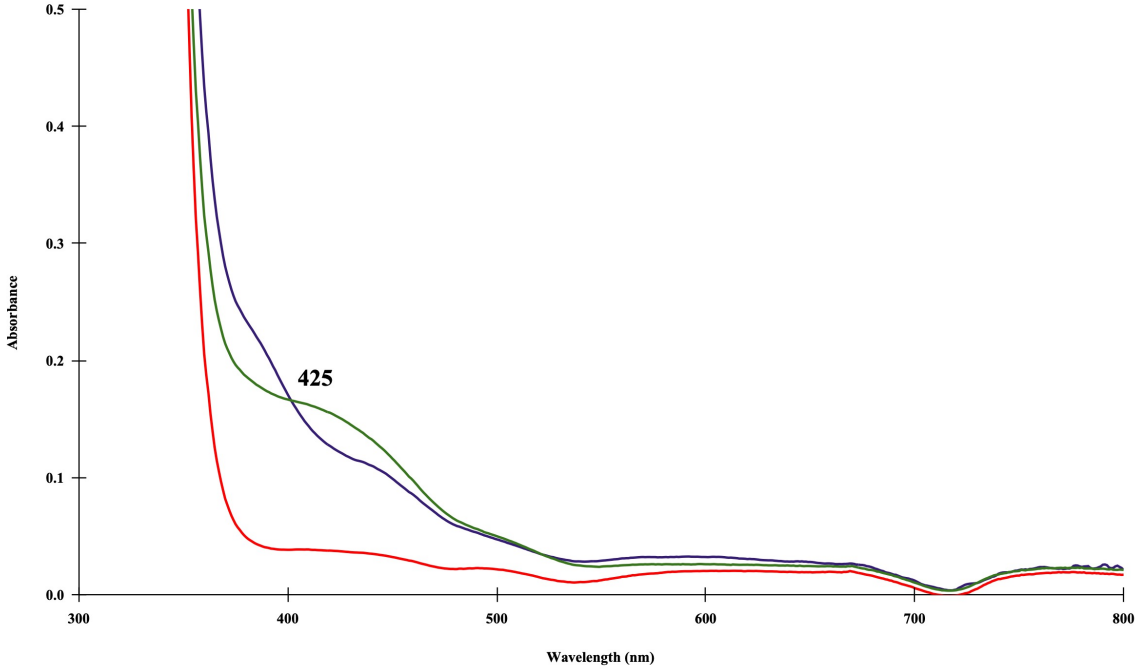

Figure S6: UV-Visible spectra for qualitative carbon monoxide assay for the reaction of **1** with 3 eq. 3DHPD substrate in MeCN following 5 minutes of oxygenation. Spectra:

negative control (red trace), positive control showing presence of the 425 nm expected shoulder (green trace), and carbon monoxide assay for the reaction (purple trace).

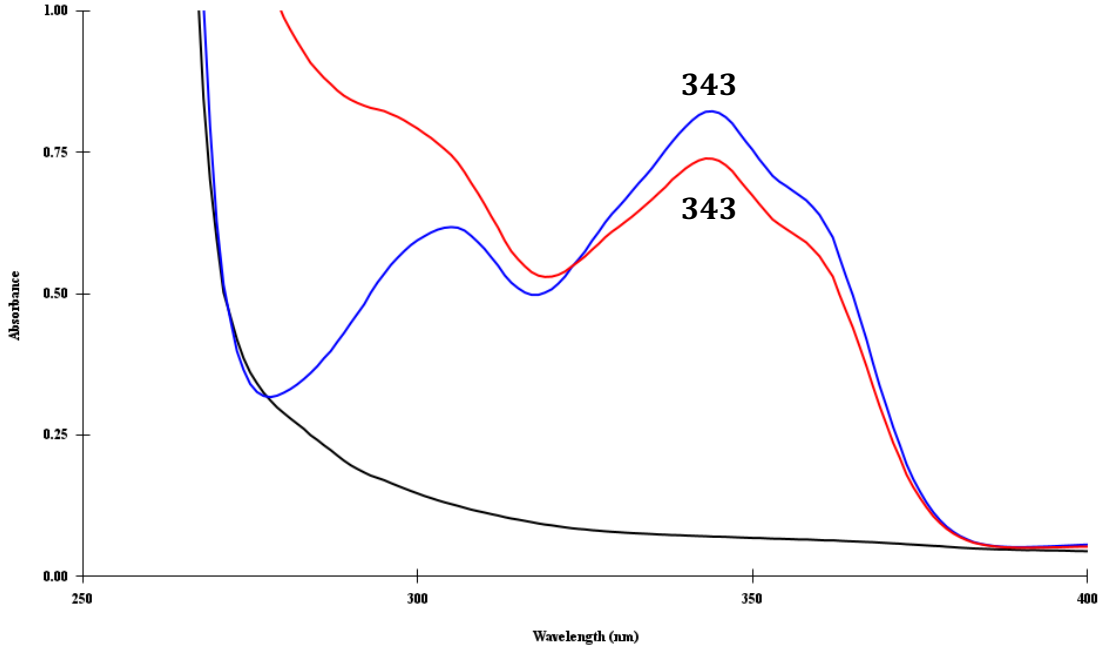

Figure S7: UV-Visible spectrum of FlaH substrate in DMF (black trace) under anerobic conditions (blue trace) and following 20 hours of continuous oxygenation at 50°C (red trace).

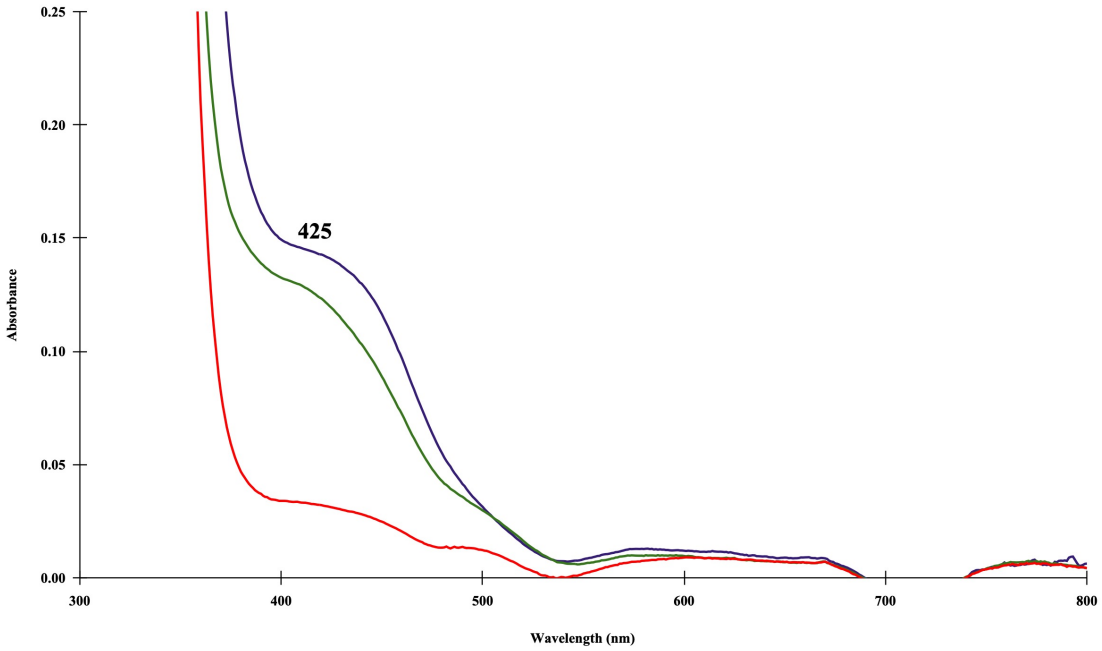

Figure S8: UV-Visible spectra for qualitative carbon monoxide assay for reaction of **1** with 1 eq. FlaH substrate in DMF under 20 hours of continuous oxygenation at 50°C. Spectra: negative control (red trace), positive control (green trace), and carbon monoxide assay for reaction (purple trace).

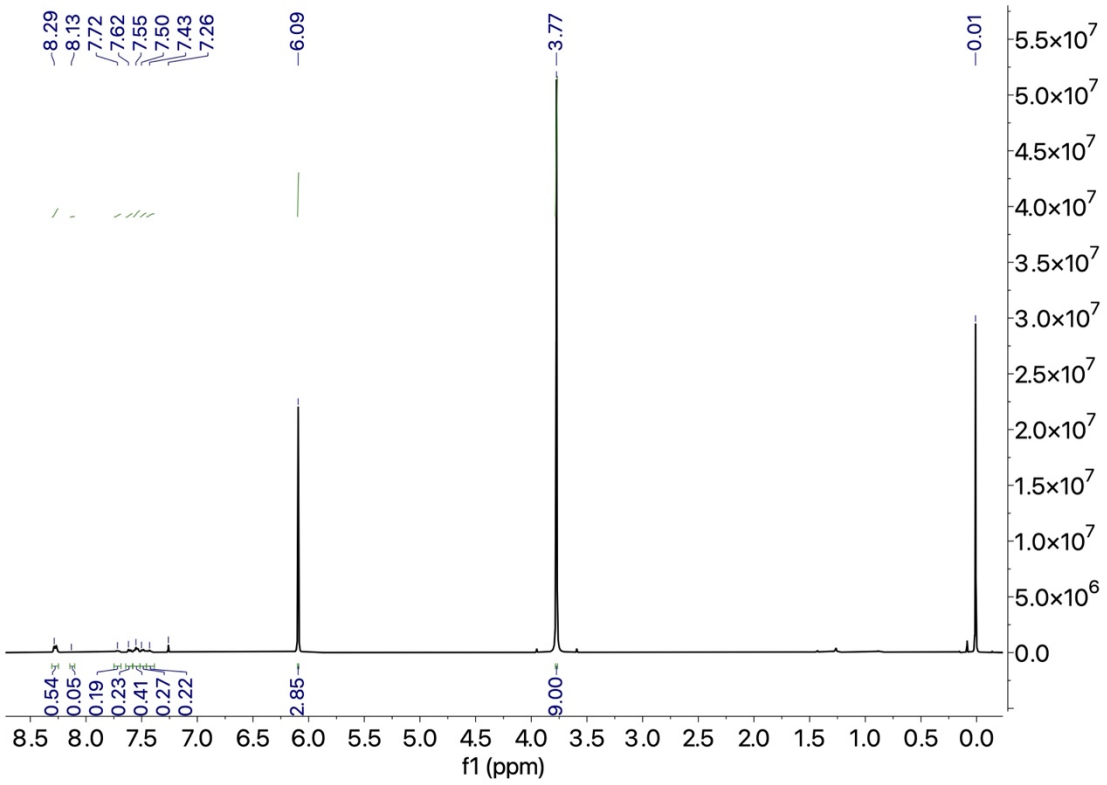

Figure S9: Quantitative ^{1}H-NMR spectrum from reaction of 1 eq. FlaH and excess O_2 at 50°C after spiking with 34.7 mg 1,3,5-trimethoxybenzne. The yield of the depside o-benzoyl salicylate was 88.5%.

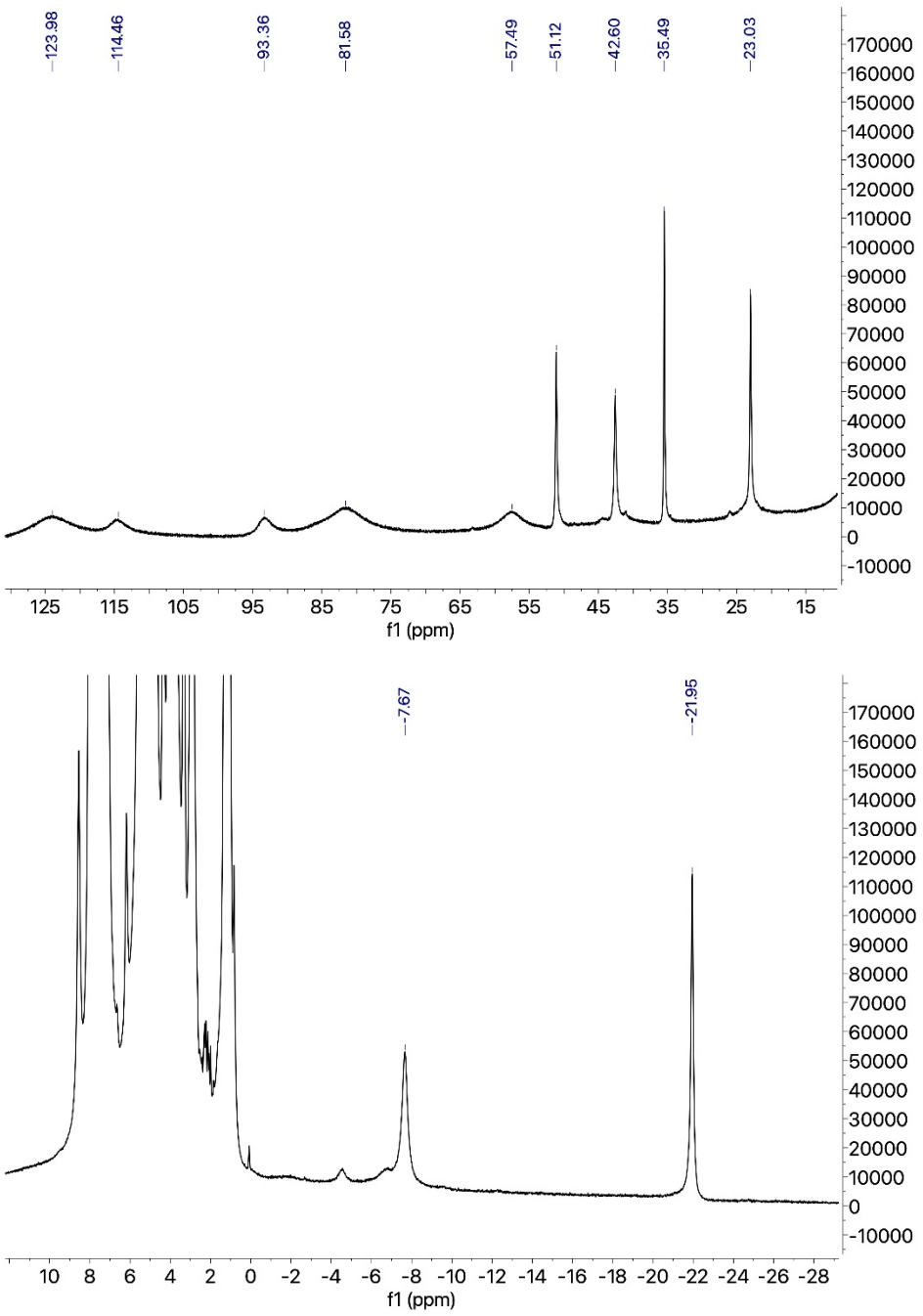

Figure S10: Paramagnetic ^{1}H-NMR of **1** following addition of 2HAPH substrate and NEt_3 under anaerobic conditions in CD_3OD.

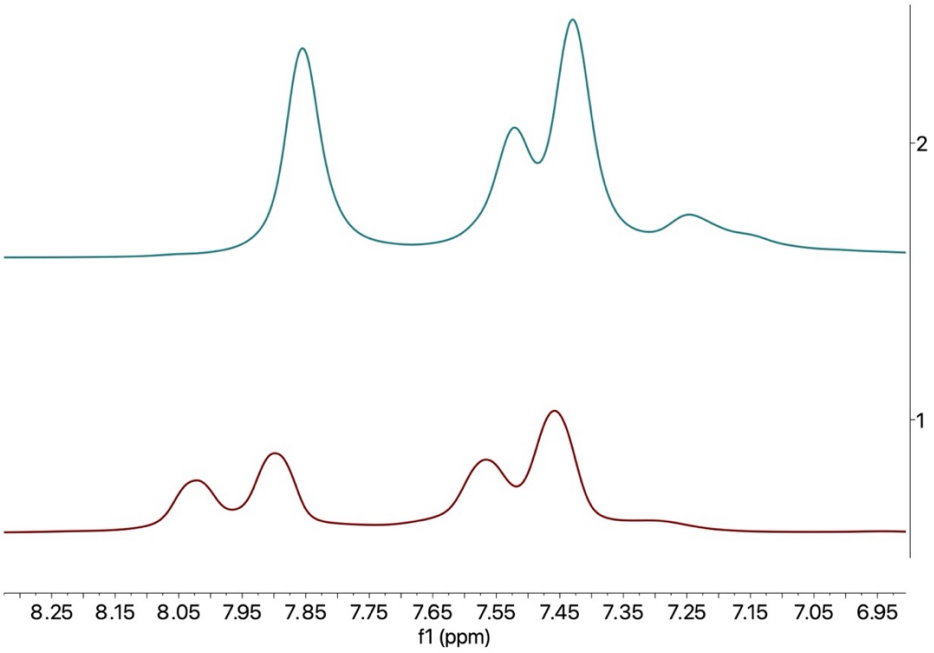

Figure S11: ^{1}H-NMR of the diamagnetic region of **1** in the presence of 2HAPH and NEt_3 before (top trace) and after (bottom trace) addition of O_2 in CD_3OD.

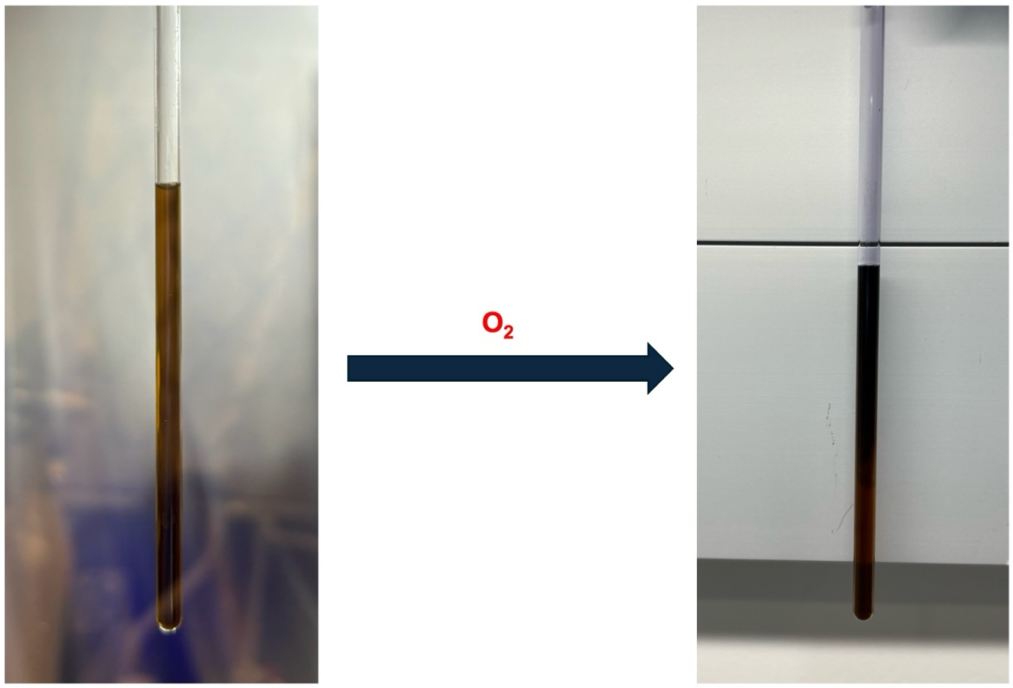

Image S3: Images of anerobic **1**-2HAPH (left) with NEt_3 and **1**-2HAPH after addition of O_2 (right).

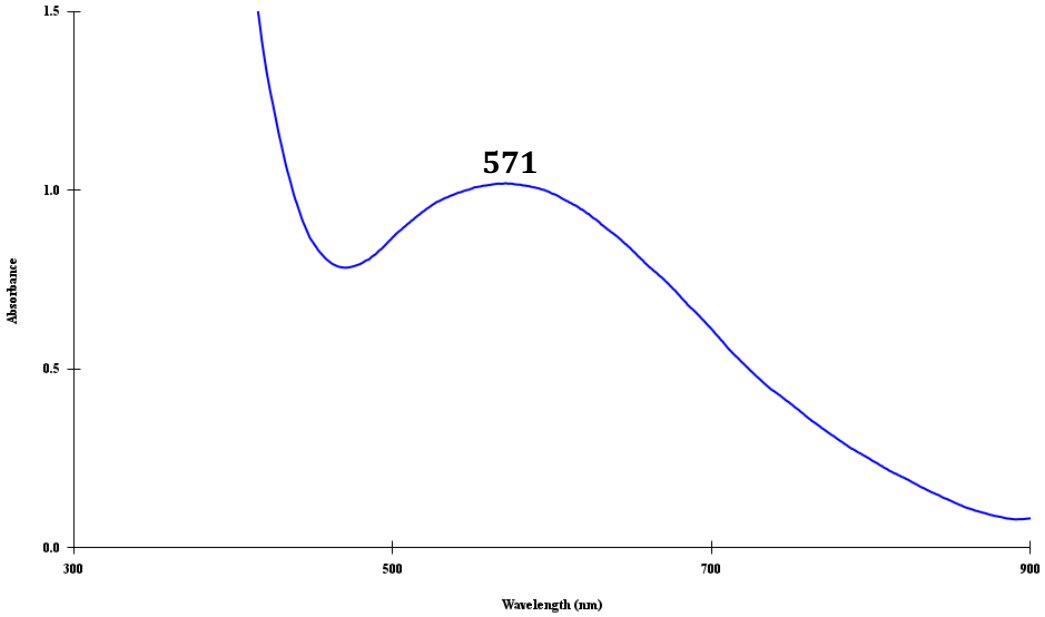

Figure S12: UV-Visible spectrum during the dioxygenation reaction of **1**-2HAPH in the presence of NEt_3 in CD_3OD (aliquot from NMR experiment).

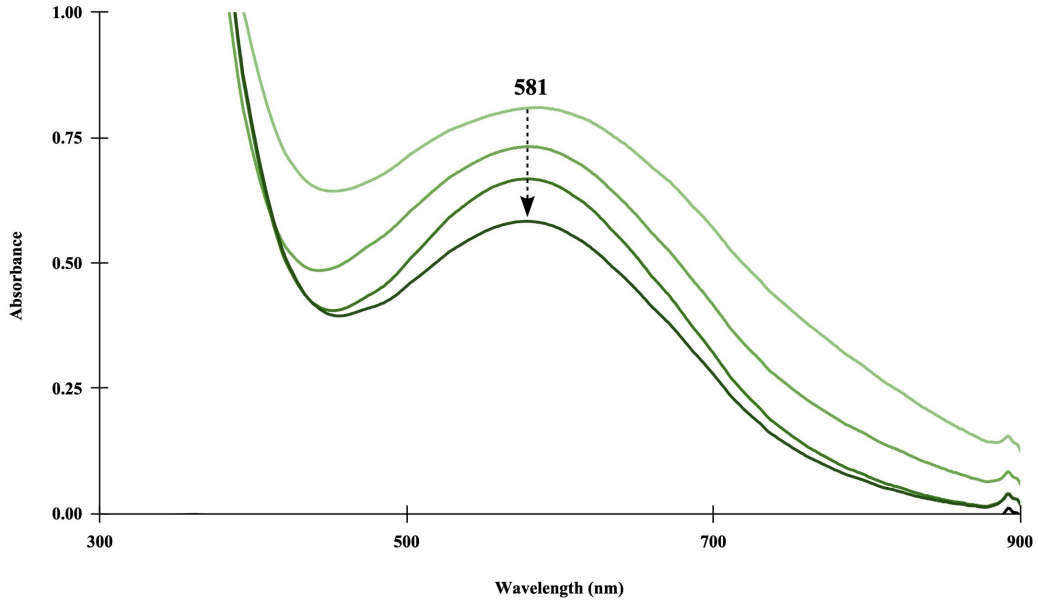

Figure S13: Timelapse UV-Visible spectrum showing monitoring the 581 nm band of the dioxygenation C-C cleavage reaction of 2HAPH mediated by **1** in MeCN at room temperature. UV-Visible traces were recorded at 6.5, 21, 52, and 72 hours post-oxygenation (green traces, increasing in darkness).

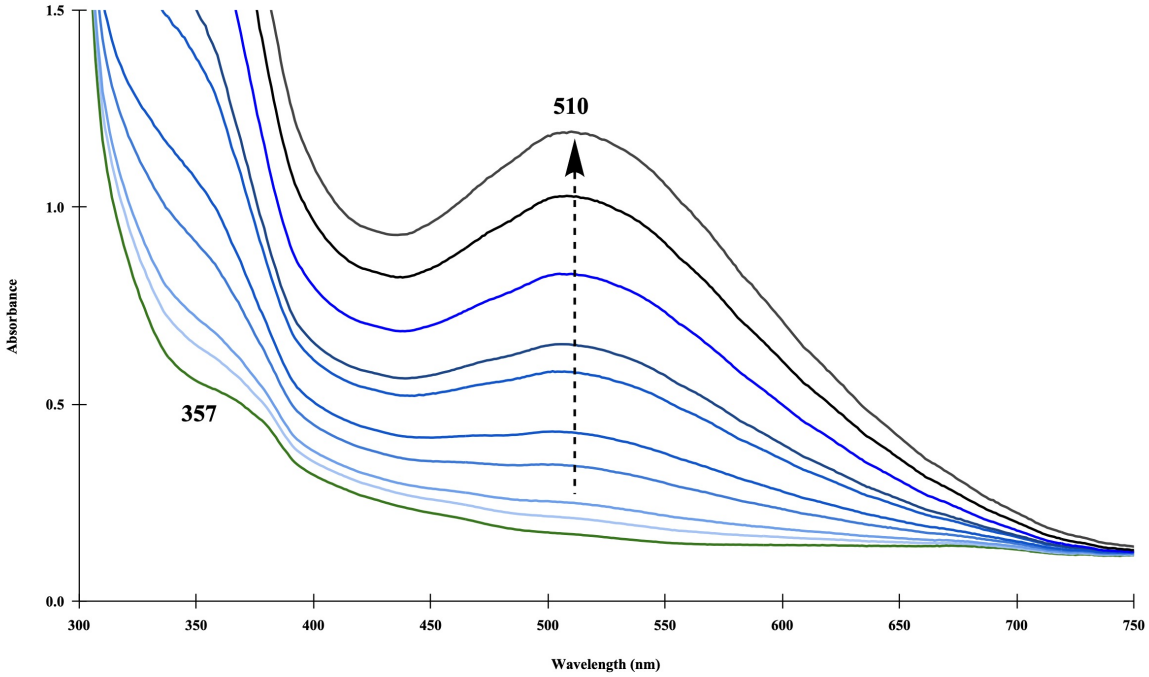

Figure S14: Time lapse (160 min), low temperature UV-Visible spectrum of the reaction of **1** with 20 eq. 2HAPH, 2 eq. NEt_3, and 0.5 eq. O_2 at -40°C in MeCN. Reaction temperature was gradually raised to 25°C after 100 minutes.

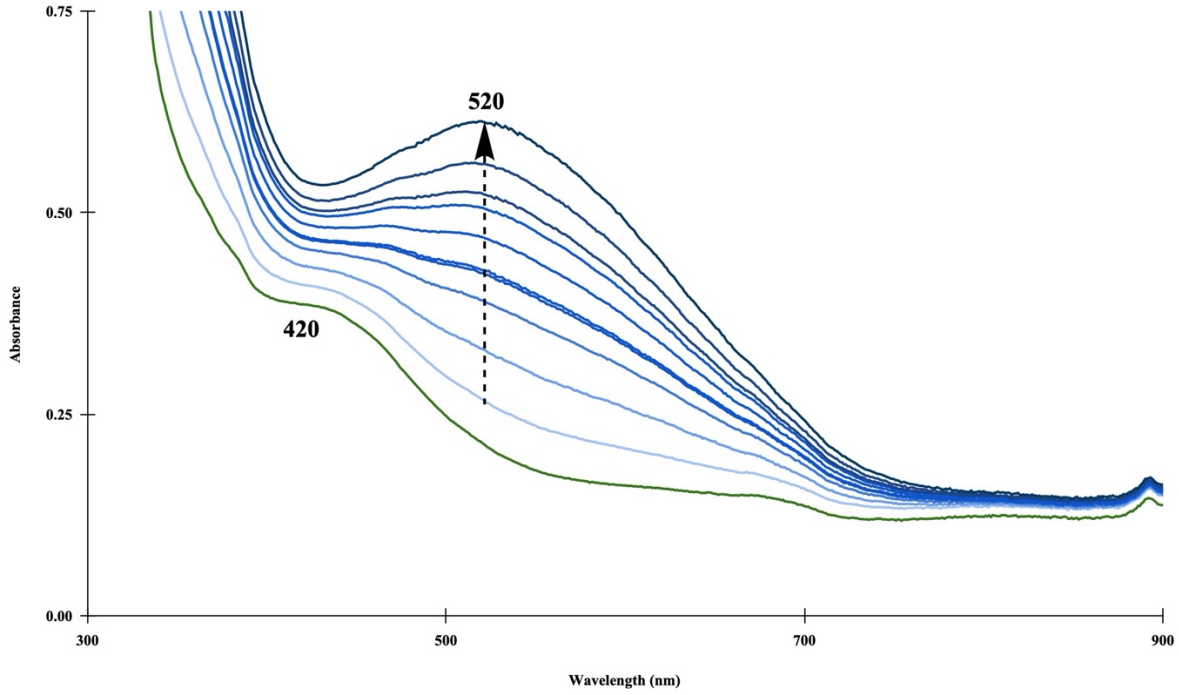

Figure S15: Time lapse (20 min), low temperature UV-Visible spectrum of the reaction of **1** with 20 eq. 2HAPH, 2 eq. NEt_3, and 10 eq. O_2 at -80°C in Acetone.

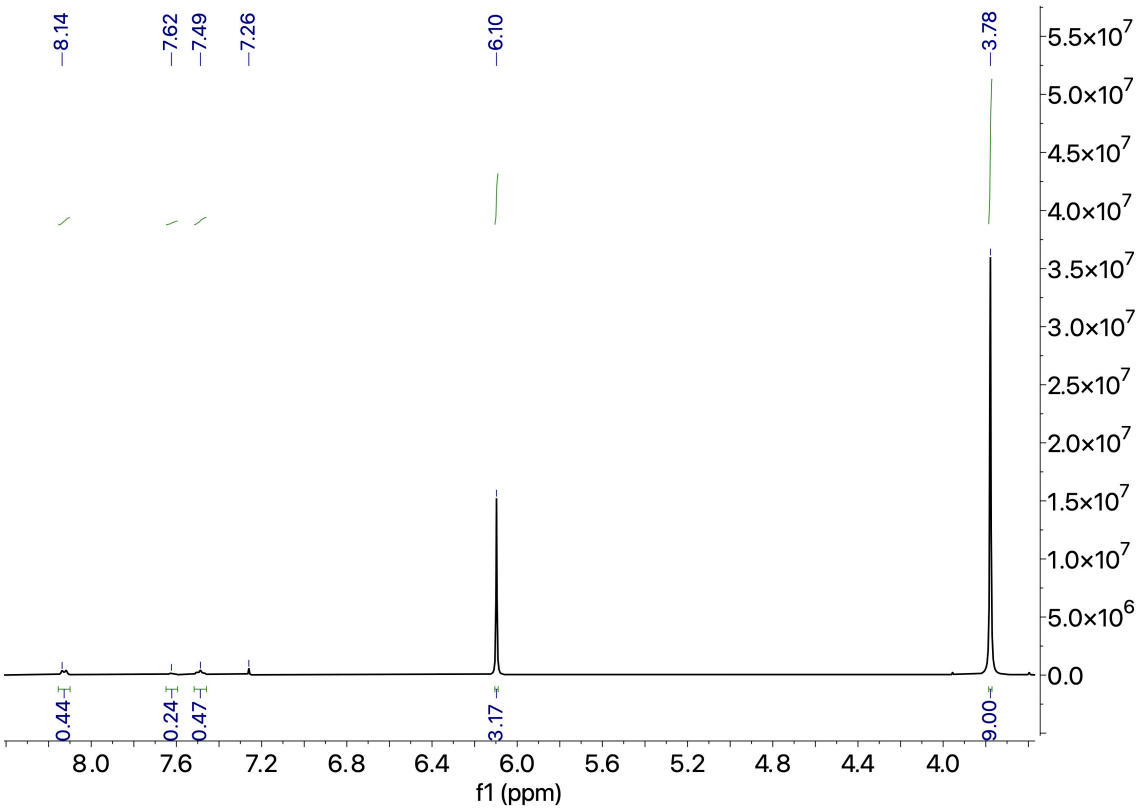

Figure S16: Quantitative ^{1}H-NMR spectrum from the reaction of 1 eq. 2HAPH, 1 eq. NEt_3, and excess O_2 after spiking with 27.9 mg 1,3,5-trimethoxybenzne. The yield of benzoic acid was 66.2%.

Synthesis, characterization, and reactivity of the ferric analogue of 1 and ferric μ-oxo dimer

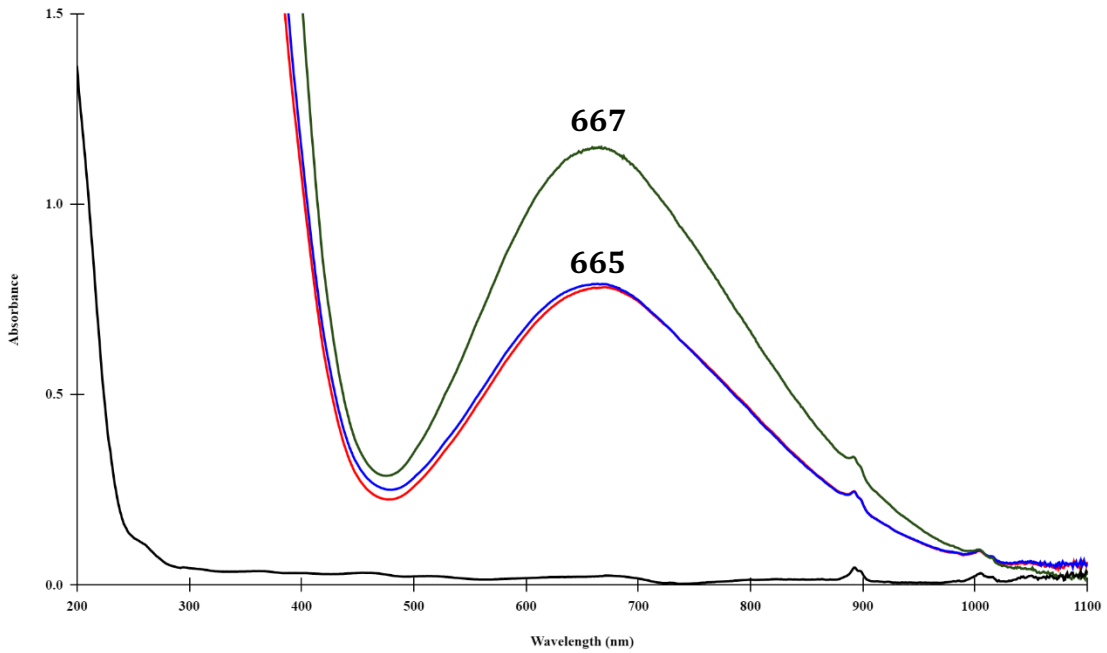

Figure S17: UV-Visible spectrum of complex **1** with Magic Blue in the presence of 1 eqv. Benzoate (green trace), 20 eqv. 2HAPH (blue trace), and without substrate (red trace) in MeCN.

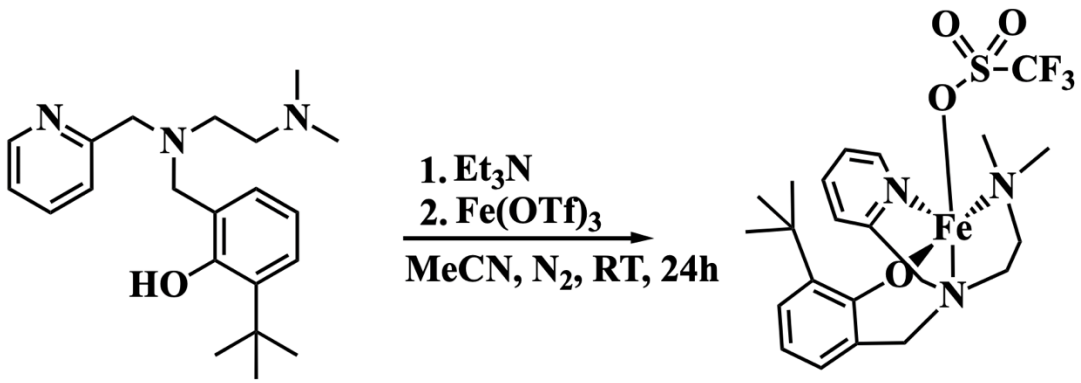

Scheme S1: Synthetic scheme for the ferric analog of **1**. The synthesis and purification of this compound were performed identically to that of **1,** except for the use of $Fe(OTf)_3$ in place of $Fe(OTf)_2$. The product is a deep blue powder in good yields.

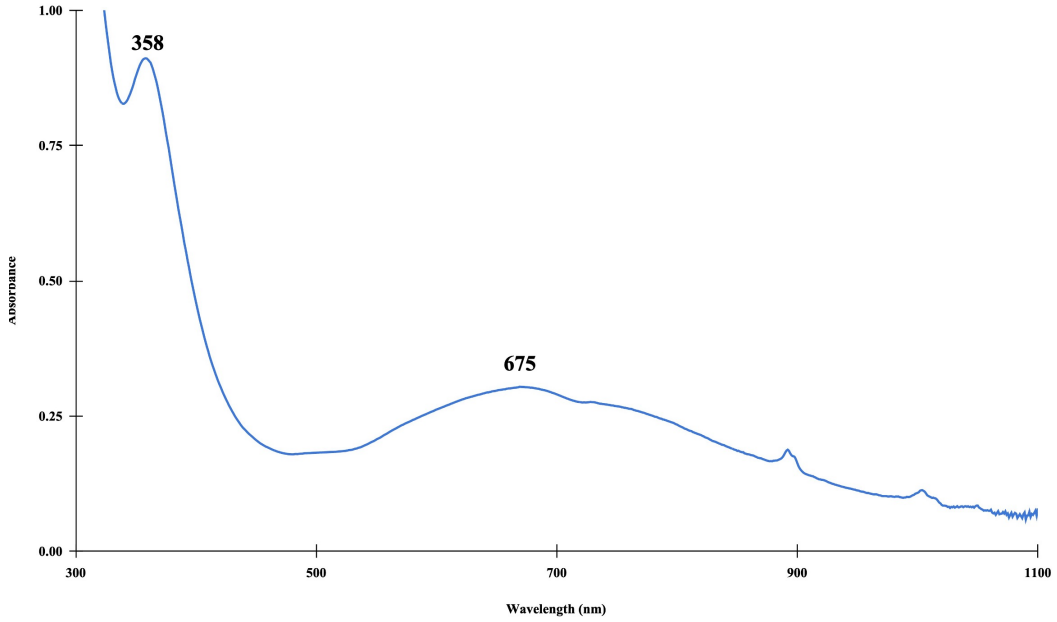

Figure S18: UV-Visible spectrum of independently synthesized ferric analog of **1** in MeCN.

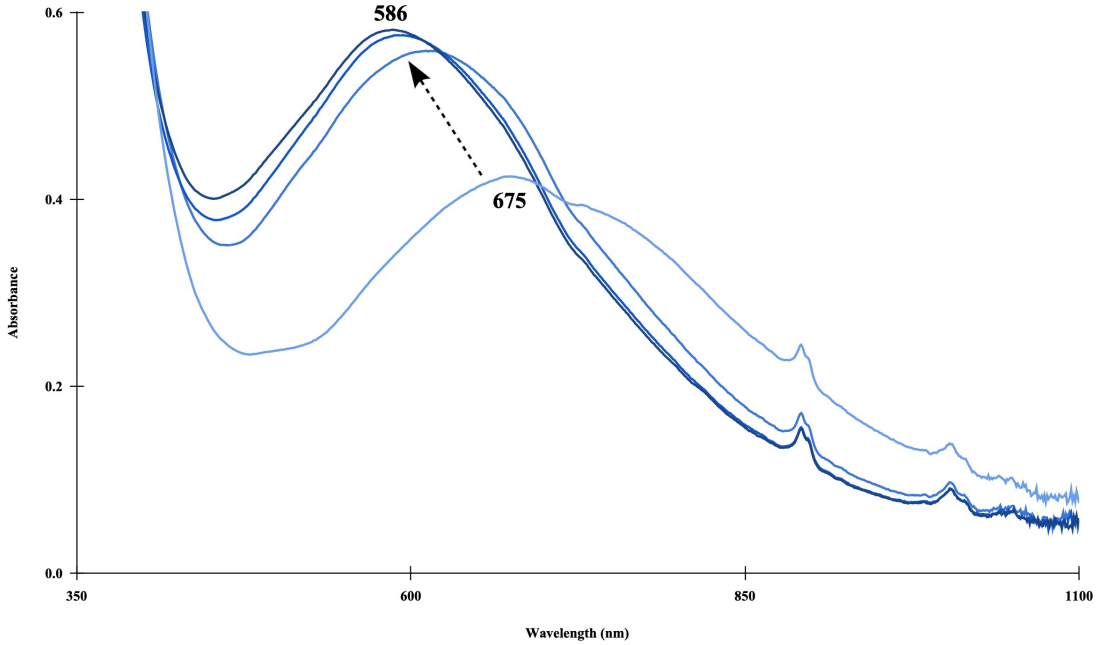

Figure S19: UV-Visible spectrum of ferric analog of **1** upon addition of tetrabutylammonium benzoate (1, 5, and 10 equivalents) in MeCN.

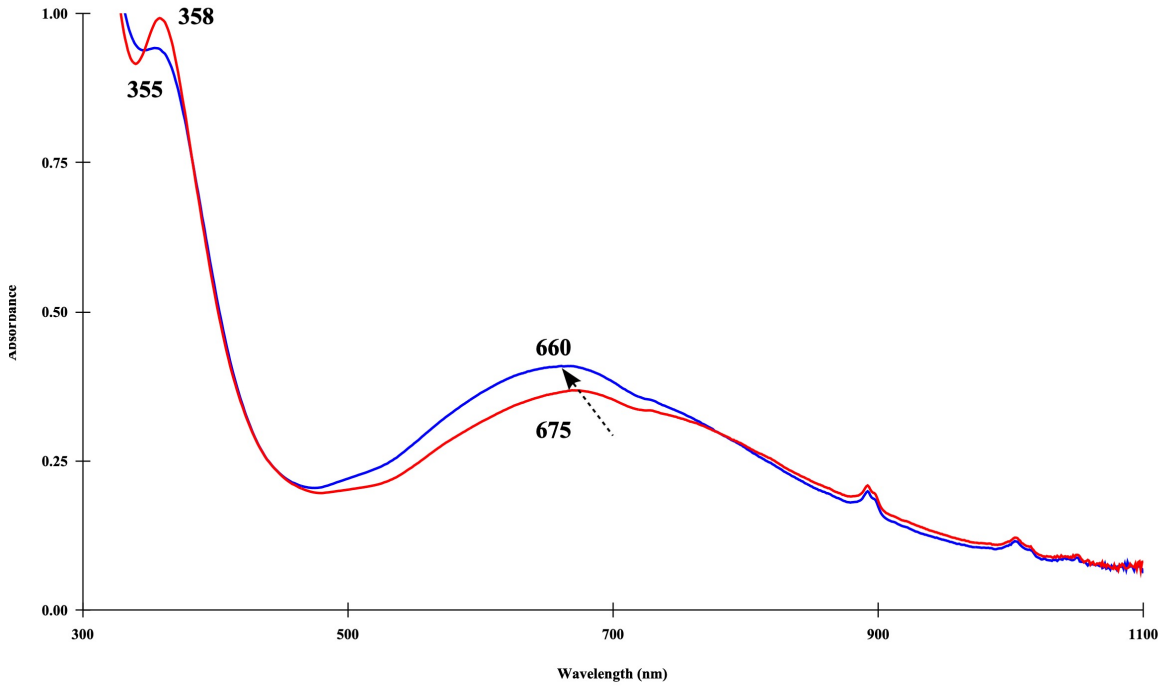

Figure S20: UV-Visible spectrum of ferric analog of **1** (red trace) upon addition of 5 eq. 2HAPH and 2 eq. NEt_3 in MeCN (blue trace).

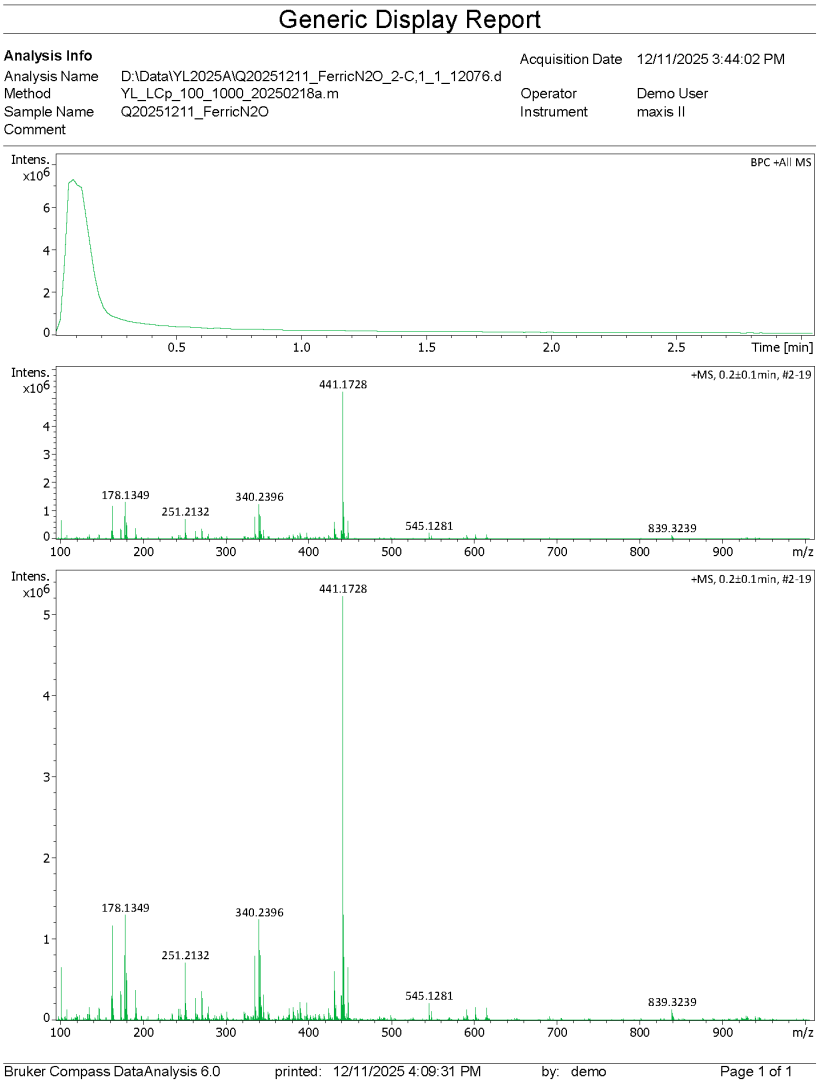

Image S4: ESI-MS of an authentic powder sample of the synthesized ferric analog of **1.** The calculated mass for the ferric analogue of **1** is 545.3 g/mol. The most prominent peak in the ESI above shows a peak at 441.1728 m/z and a minor peak at 545.1259 m/z. Similar to the ESI of **1** (Image S2), the first one corresponds to the addition of a mass of 45 mass units, which we attribute to the binding of formate (45 g/mol) to the ferric analogue of **1**. The m/z at 545 indicates a ferric triflate-bound complex. The presence of formate is not unusual in the spectrometer that is normally connected to an LC instrument.

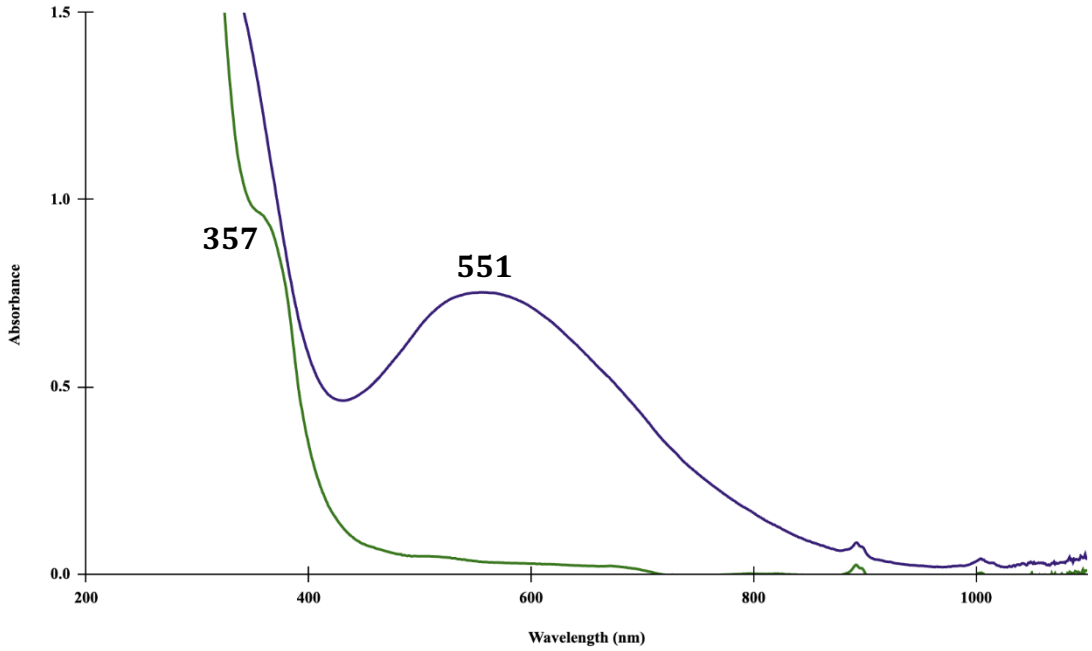

Figure S21: UV-vis spectrum of **1** under anaerobic conditions (green) and excess O_2 (purple) in MeCN. This reaction yields a purple species that is indefinitely stable at room temperature.

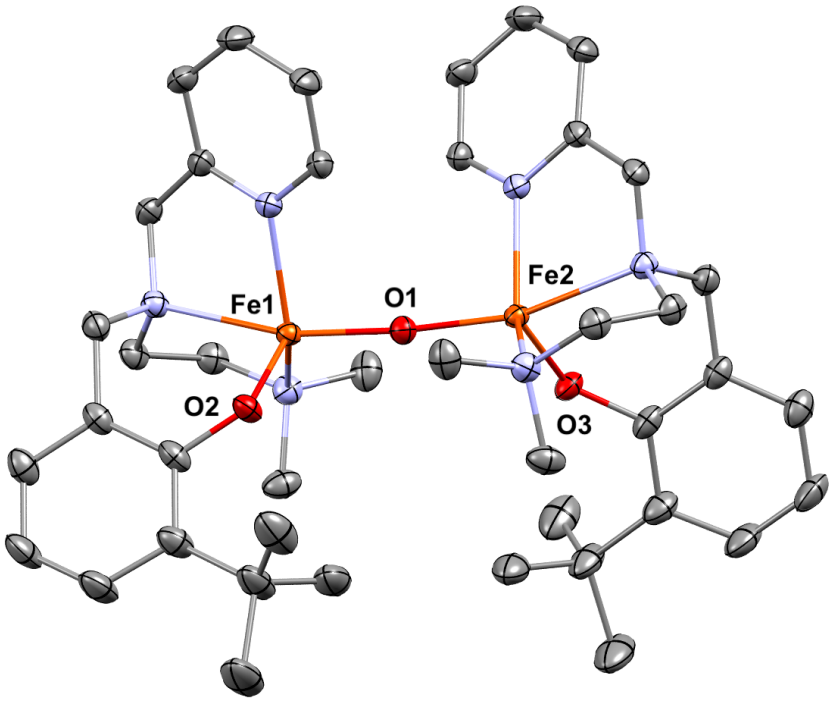

Figure S22: ORTEP representations of the crystal structure of ferric μ-oxo dimer derived from reactions of **1** and O_2 with ellipsoids drawn at the 50% probability level. H atoms and both triflate counterions were omitted from the figure for clarity.

Synthesis of $Fe_2(N_3O_2)$-μ-O](OTf)$_2$, μ-oxo dimer: An excess (5-minute bubbling) of dry O_2 gas was added to a solution of 150 mg of **1** in 5ml of dry and degassed acetonitrile (5.5 mM). The color change from green to purple is immediate. The solvent was removed under vacuum, and the resulting purple oily residue was brought into a glove box for workup. The oil was washed 4x with diethyl ether, resulting in a purple residue. This residue was further dried under vacuum for 1 hr. The dry resulting powder was reversed layered with THF as the solvent and Toluene as the anti-solvent. The mixture was allowed to sit for several days in a freezer at a temperature of -10 °C. After this time, large, rhombic purple crystals resulted.

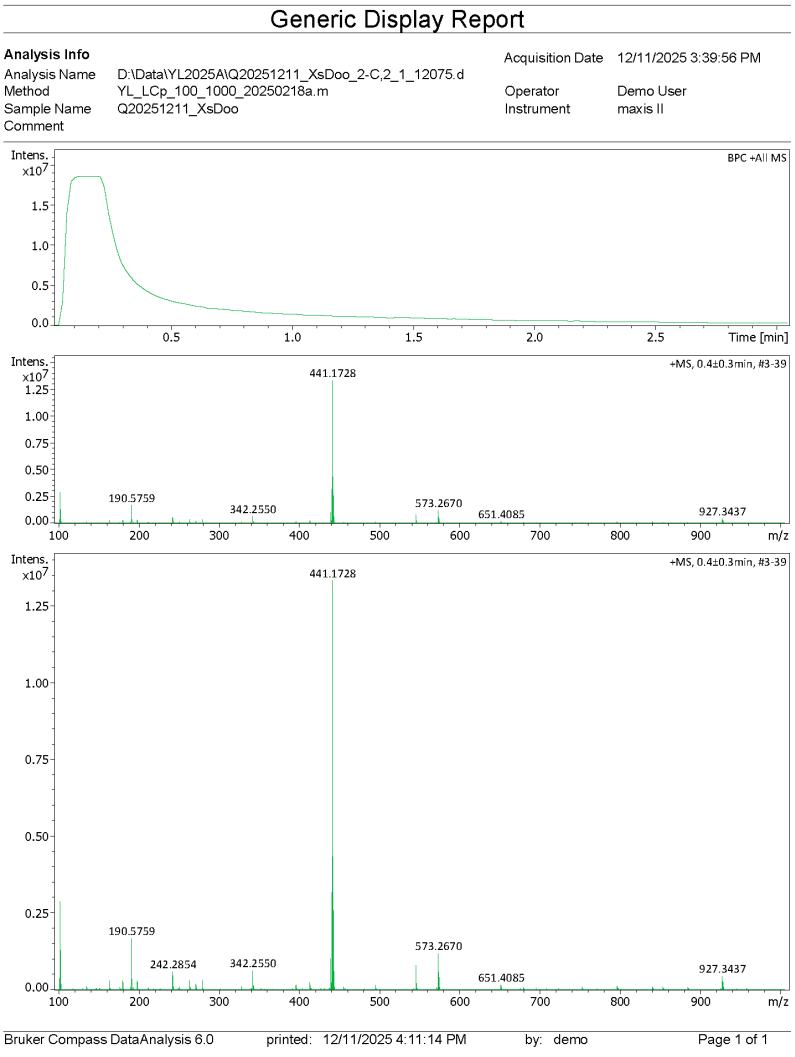

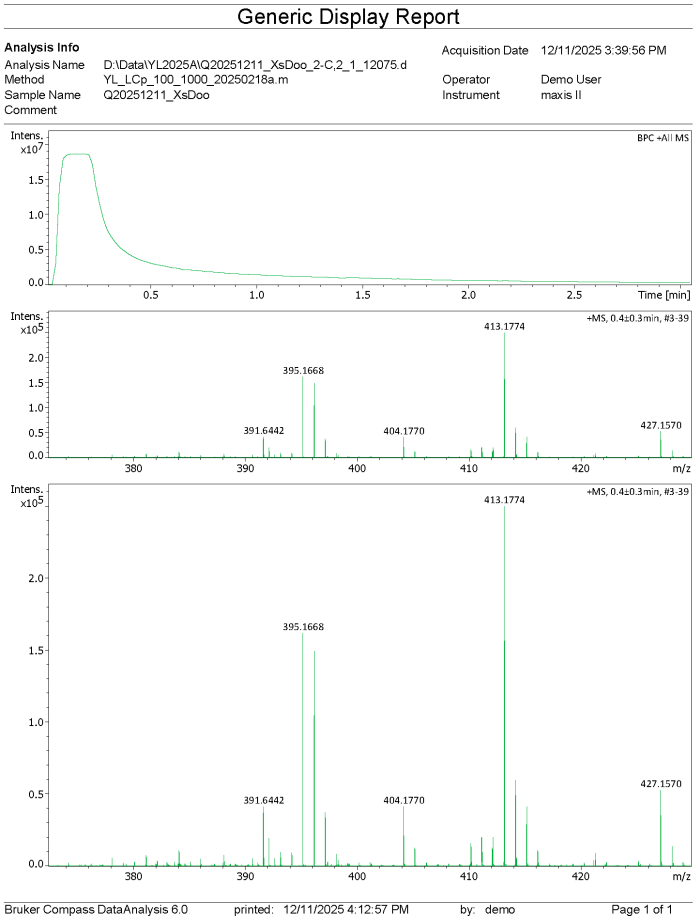

Image S5: ESI-MS of ferric μ-oxo dimer isolated as a clean powder, which was derived from the reaction of **1** with $\mathbf{O_2}$. The calculated mass for the ferric μ-oxo dimer is 808.6 g/mol, with a charge of +2. The most prominent peak in the ESI (top picture above) shows a peak at 441.1728 m/z and a minor peak at 573.267 m/z. Like the ESI of **1** (Figure S2), and the ferric analogue of **1** (Figure S4). The peak at 441 m/z corresponds to the addition of a mass of 45 mass units, which we attribute to the binding of formate (45 g/mol) to the ferric analogue of **1**. The peak at 573 m/z is not identified. The ferric μ-oxo dimer should show a peak m/z (where z +2) at 404 mass units. The bottom set of pictures, above, shows the presence of this peak, albeit at much lower intensity ($x10^5$). Additionally, in this same intensity range, we observe a peak at 413 m/z, which corresponds to a gain of 17 mass units. This peak could correspond to a protonated oxo ligand, i.e., hydroxide, bound to a ferric analogue of **1** (charge +1).

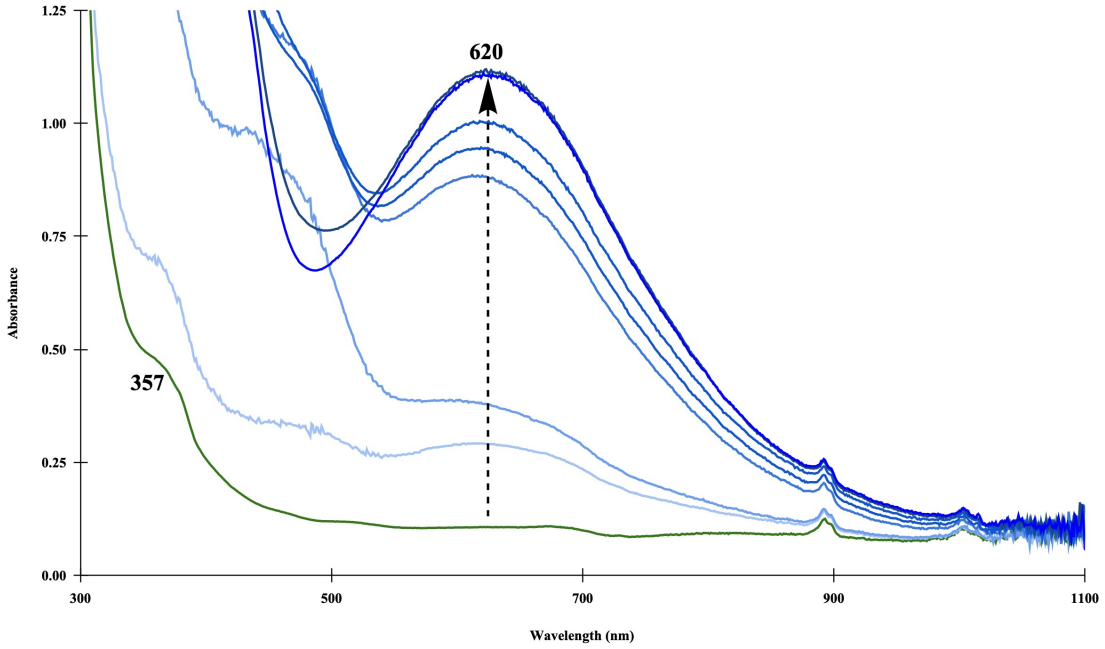

Figure S23: Time lapse (10 min), low temperature UV-Visible spectrum of the reaction of **1** with 1 eq. mCPBA at -40°C in MeCN producing a 620 nm absorption band. This band persists at room temperature.

A

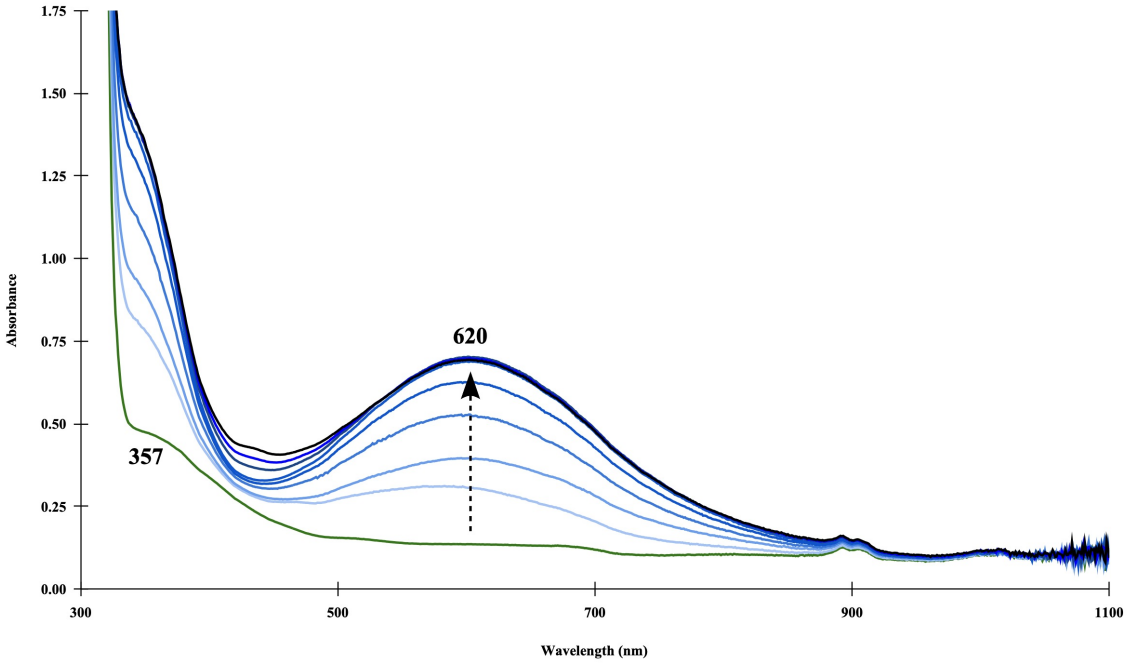

B

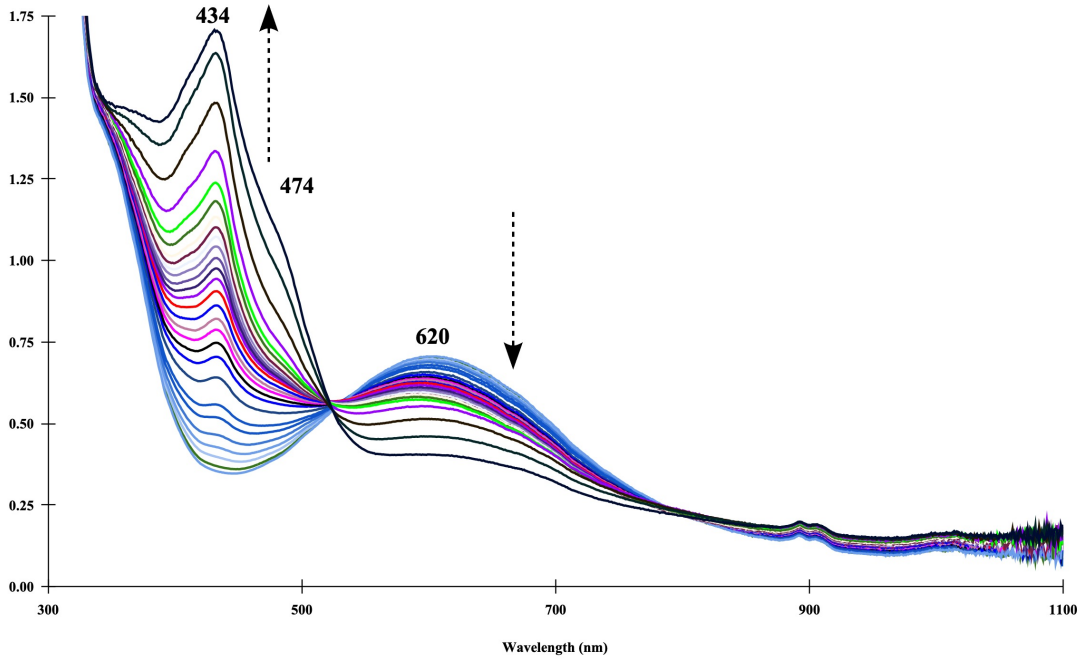

C

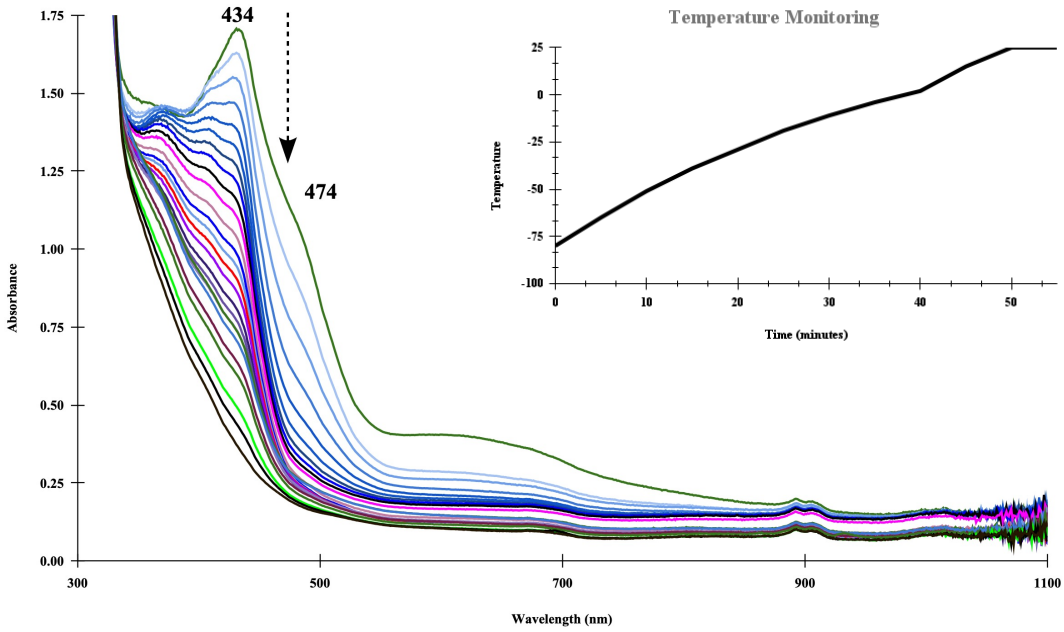

Figure S24: Time lapse (90 min), low temperature UV-Visible spectrum of the reaction of **1** with 6 eq. mCPBA at -80°C in Acetone. **A.** Initial growth phase (time = 6 min.). This phase presumably corresponds to the formation of a 1-electron oxidized ferric species. Consistent with our observations in the experiments depicted in figures S18-20. **B.** The

ferric species undergoes an isosbestic transformation to a second transient species with intense absorption bands at 434 and 474 (sh) nm. **C.** Monitoring of the warming of the solution over the course of 60 min. when the reaction was gradually warmed up to room temperature (inset plot of time vs. temperature change). The intermediate from part **B** decays entirely during this time.

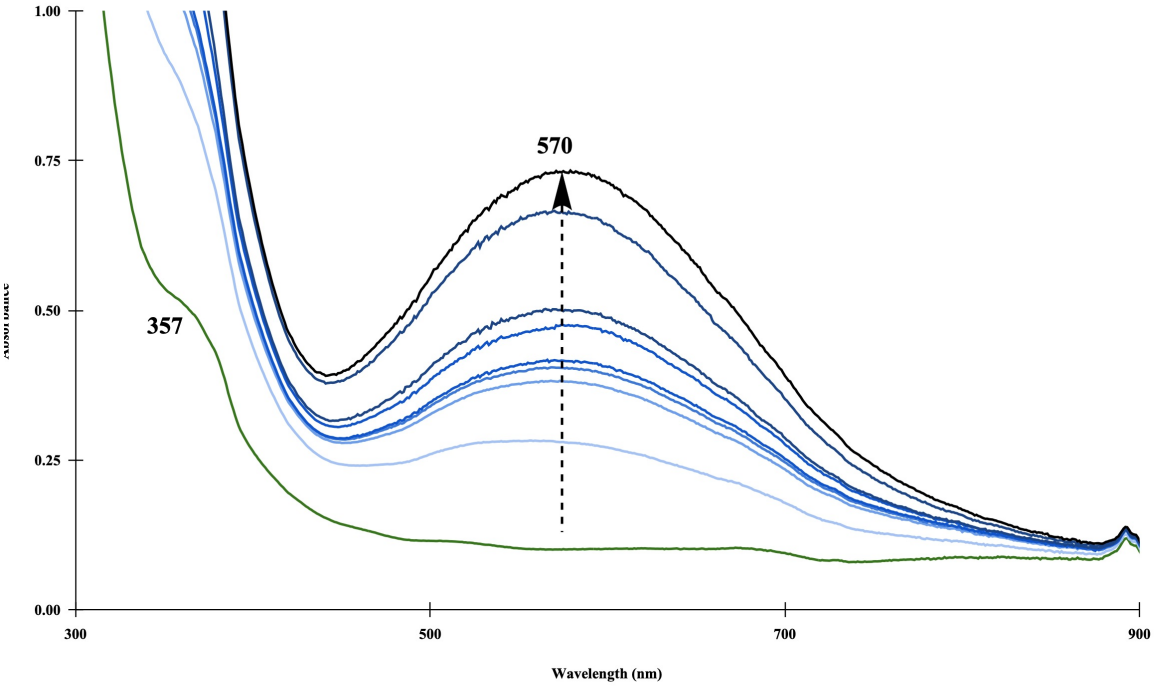

Figure S25: Time lapse (2.5 min), low temperature UV-Visible spectrum of the reaction of **1** with excess O_2 at -40°C in MeCN.

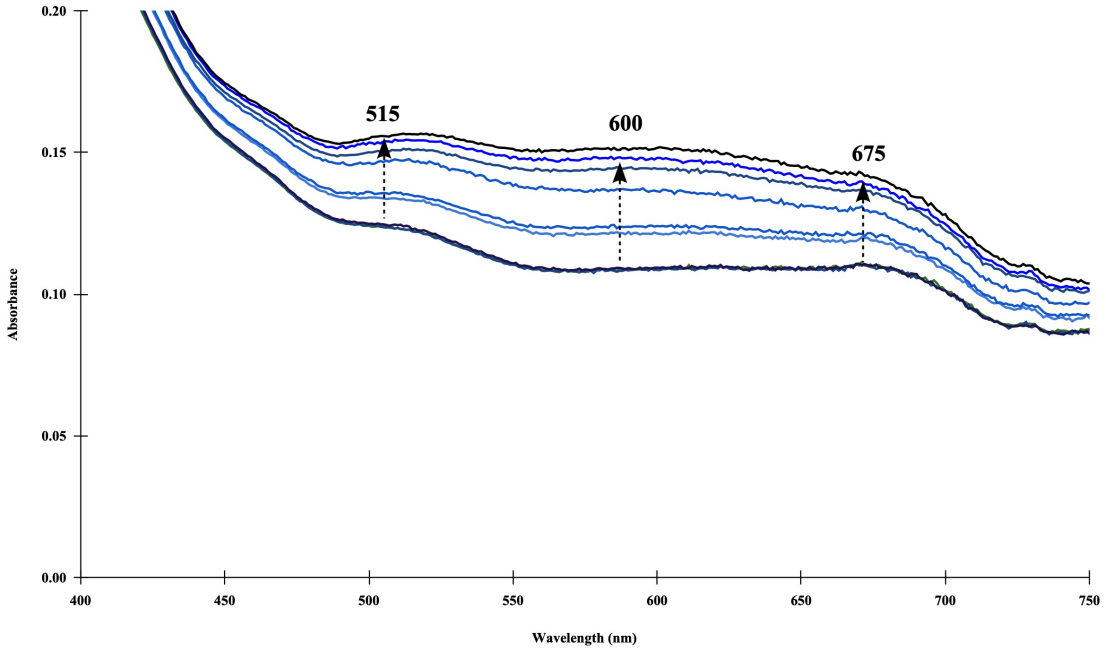

Figure S26: Time lapse (2.5 min), low temperature UV-Visible spectrum of the reaction of **1** with 0.5 eq. O_2 at -40°C in MeCN.

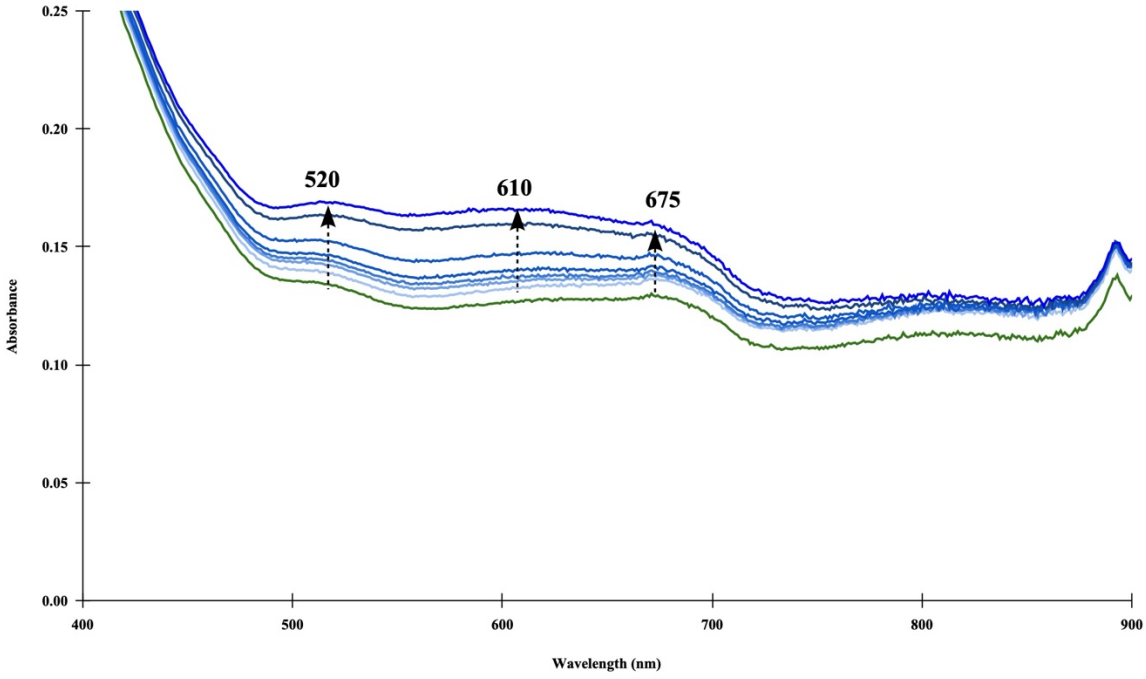

Figure S27: Time lapse (20 min), low temperature UV-Visible spectrum of the reaction of **1** with 1 eq. O_2 at -80°C in acetone.

Computational calculations

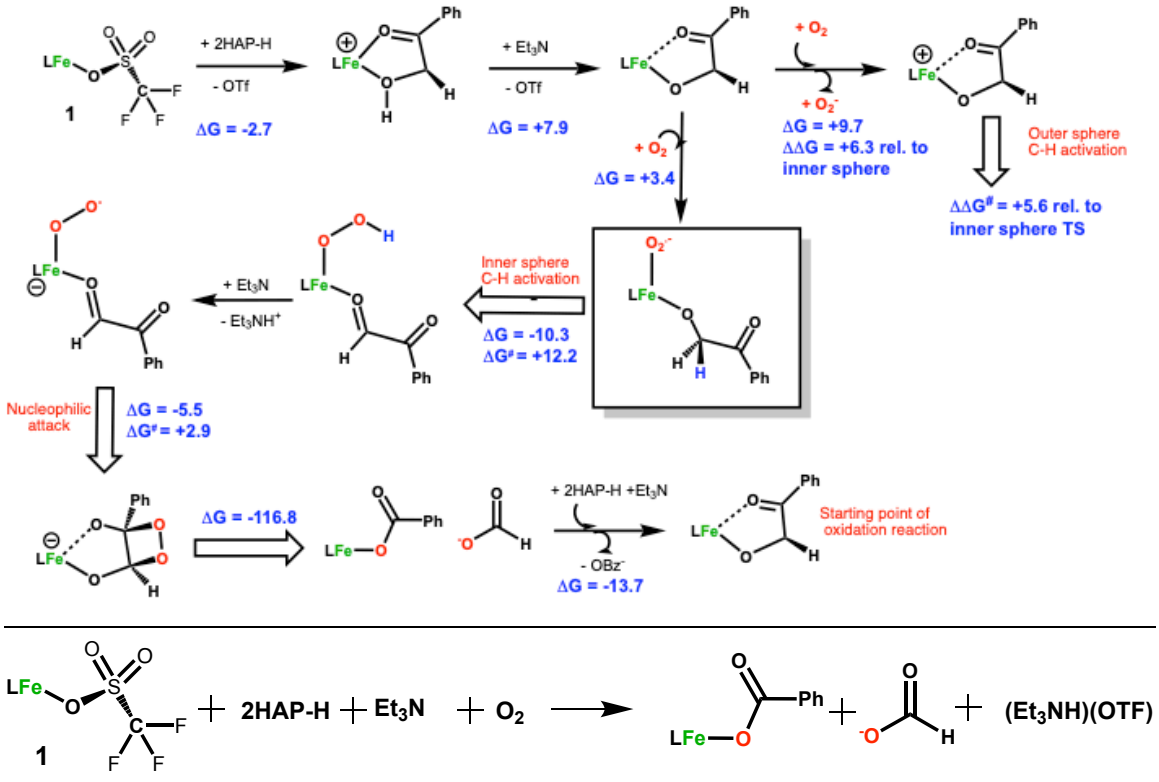

Figure S28. Proposed DFT-derived mechanism of O_2 activation and C-C bond cleaving of 2-HAPH. The balanced chemical equation for the reaction was added for clarity.

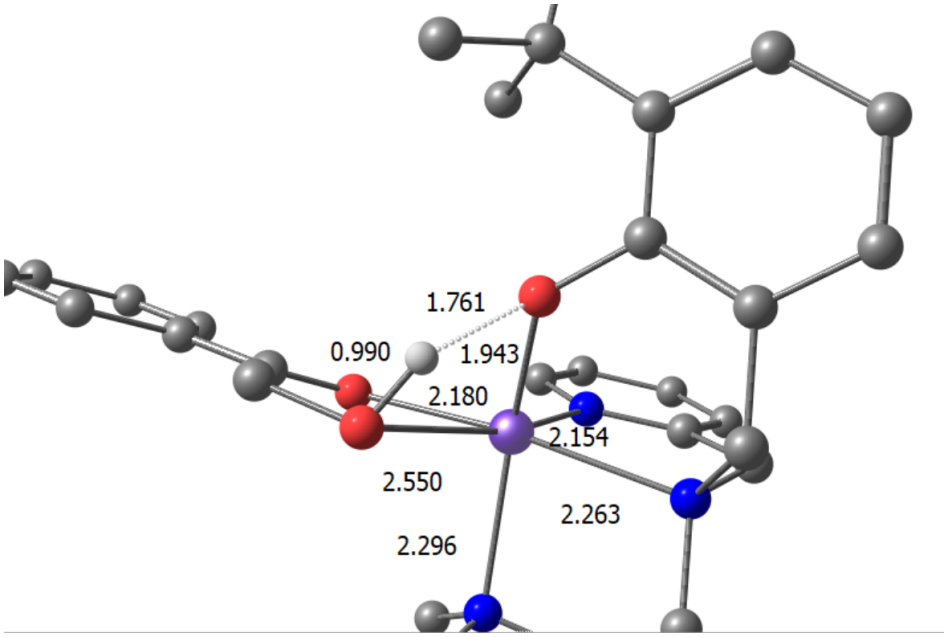

Figure S29. Core geometry of cationic, S = 2, Fe(N_3O)(2HAPH) complex.

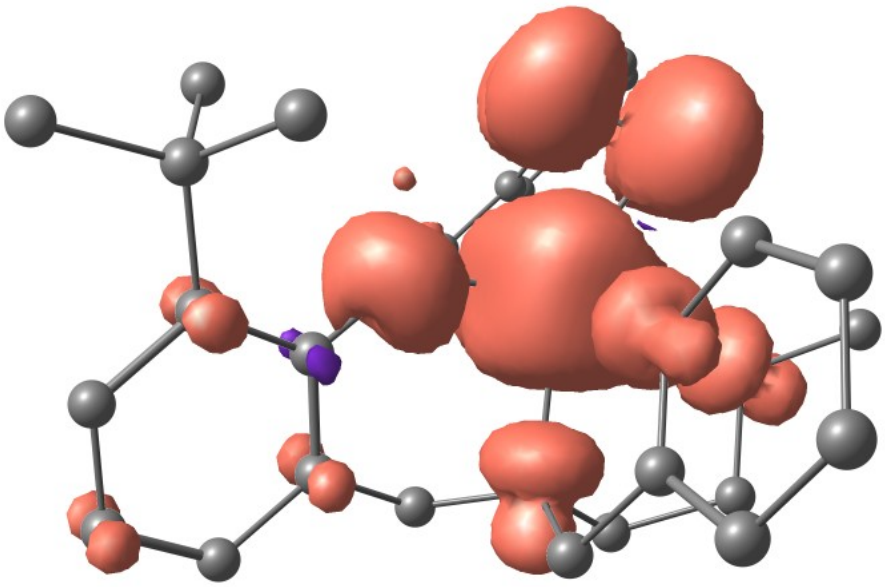

Figure S30: Calculated spin density (IsoValue = 0.002 a.u.) for the Fe^{III}-superoxide complex (orange envelope indicates positive spin density.

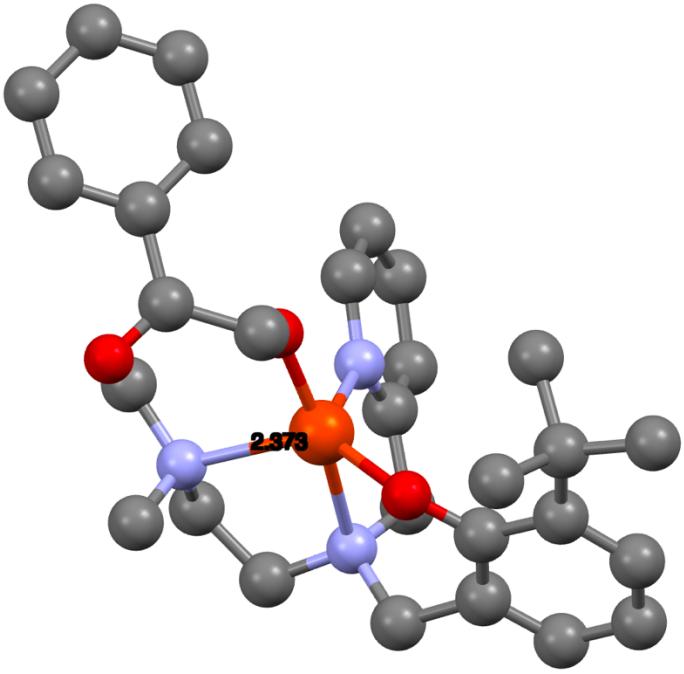

Figure S31: Calculated geometry for 1 bound to $2HAP^-$ in a k-1configuration. The bond length between the Fe(II) and the NMe_2 moiety of the ligand is 2.373 Å.

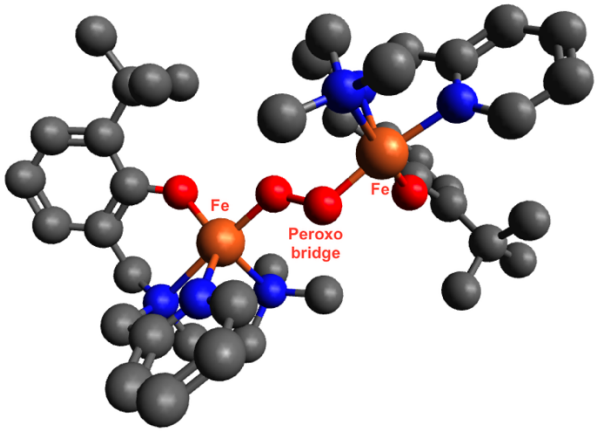

A.

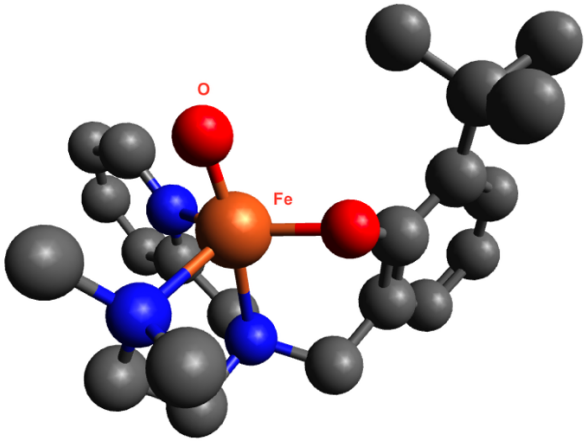

B.

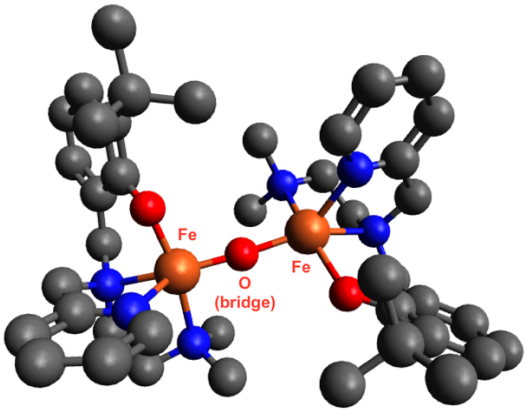

C.

$Fe(II)\text{-}OTf + O_2 = [Fe(III)\text{-}O_2]^+ + OTf^-$	10.86
$[Fe(III)\text{-}O_2]^+ + Fe(II)\text{-}OTf = [Fe\text{-}OO\text{-}Fe]^{2+} + OTf^-$	1.78
$[Fe(III)\text{-}OO\text{-}Fe(III)]^{2+} = 2\ [Fe(IV)=O]^+$	-4.29
$[Fe(IV)=O]^+ + Fe(II)\text{-}OTf = [Fe(III)\text{-}O\text{-}Fe(III)]^{2+} + OTf^-$	0.56

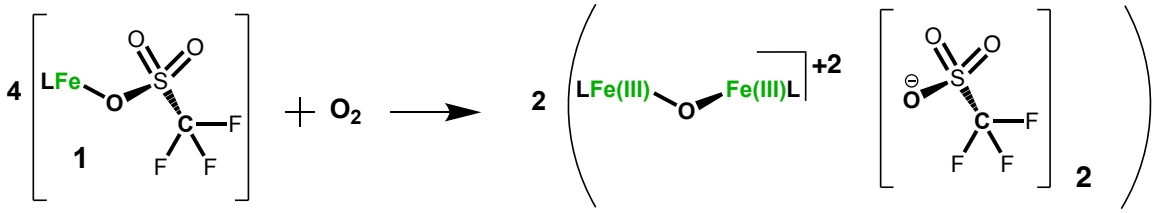

Figure S32: Calculated structures for the key intermediates resulting from the reaction between compound **1** and O_2. **A.** Fe(III)-OO-Fe(III) (μ-peroxo dimer), **B.** Fe(IV)=O, and **C.** Fe(III)-O-Fe(III) (μ-oxo dimer). Corresponding ΔG values in kcal/mol for each of the balanced reactions in the proposed mechanism towards the formation of the final product (ferric-μ-oxo dimer). The balanced chemical equation for the reaction was added for clarity.

\

X-ray crystallographic studies

Experimental description: A single crystal of **1** was mounted under mineral oil on a Mitegen micromount and immediately placed in a cold nitrogen stream prior to data collection. The single crystal data was collected on a Bruker D8 Quest equipped with a Photon 3 CMOS detector and a Mo ImS source. Data were collected using a combination of phi and omega scans and integrated with the Bruker SAINT program. Structure solution was performed using the SHELXTL software suite. Intensities were corrected for Lorentz and polarization effects and an empirical absorption correction was applied using SADABS v2014/4. Non-hydrogen atoms were refined with anisotropic thermal parameters and hydrogen atoms were included in riding idealized positions.

Table S1:

Empirical formula	C22 H30 F3 Fe N3 O4 S
Formula weight	545.40
Temperature	100(2) K
Wavelength	0.71073 Å
Crystal system	Triclinic
Space group	P-1
Unit cell dimensions	a = 9.4612(15) Å a= 81.071(3)°.
b = 17.394(3) Å	b= 86.400(4)°.
c = 22.774(2) Å	g = 82.258(4)°.
Volume	3665.3(9) Å3
Z	6
Density (calculated)	1.483 Mg/m^3
Absorption coefficient	0.759 mm-1
F(000)	1704
Crystal size	0.190 x 0.152 x 0.086 mm^3
Theta range for data collection	2.174 to 28.366°.
Index ranges	-12<=h<=12, -23<=k<=23, -30<=l<=29
Reflections collected	218409
Independent reflections	18292 [R(int) = 0.0651]
Completeness to theta = 25.242°	99.9 %
Absorption correction	Semi-empirical from equivalents
Max. and min. transmission	0.95472 and 0.89900
Refinement method	Full-matrix least-squares on F2
Data / restraints / parameters	18292 / 1746 / 1128
Goodness-of-fit on F2	1.024
Final R indices [I>2sigma(I)]	R1 = 0.0340, wR2 = 0.0734
R indices (all data)	R1 = 0.0536, wR2 = 0.0816
Extinction coefficient	n/a
Largest diff. peak and hole	0.752 and -0.578 e.Å-

Crystallographic refinement details for 1: A structural model consisting of three crystallographically independent molecules of **1** per asymmetric unit was developed. The $CH_2CH_2NMe_2$ arm of one ligand is disordered over two orientations. The like C-C and C-N distances were restrained to be similar (esd 0.02Å). The triflate anions on the other two independent molecules are disordered over two orientations. The like C-F, C-S and S-O distances were restrained to be similar (esd 0.02 Å). Rigid-bond restraints were imposed on displacement parameters for all disordered sites and similar displacement amplitudes (esd 0.01) were imposed on disordered sites overlapping by less than the sum of van der Waals radii.

CCDC deposition number: 2486757

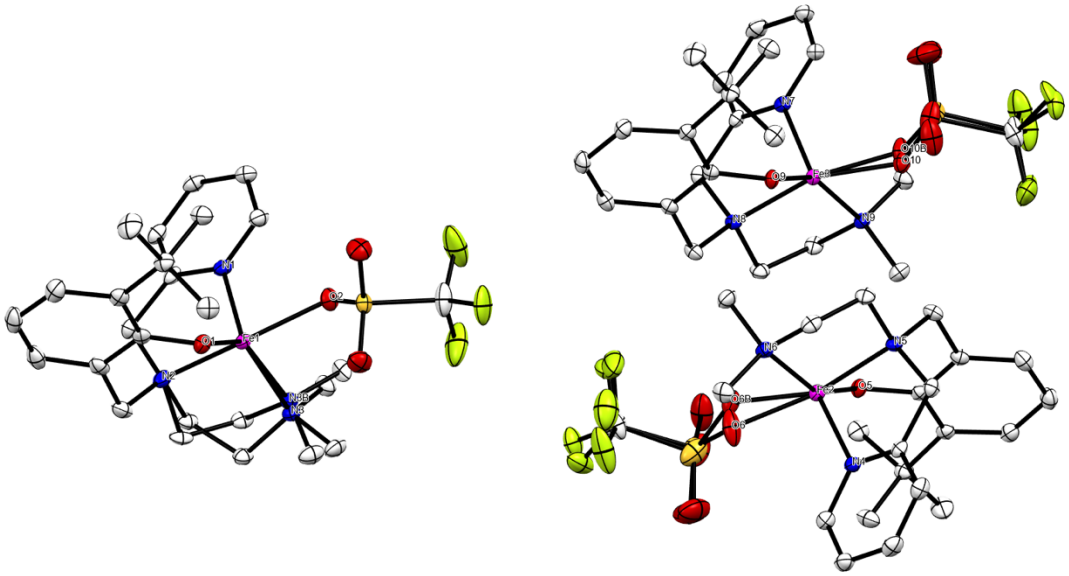

Figure S33: ORTEP representations of the crystal structure of [Fe(II)(NMe_2-6H-Py-2-t-ButPhOH)(OTf)] (**1**) with ellipsoids drawn at the 50% probability level. H atoms are omitted for clarity. All the orientations and corresponding disorders from the original structure are shown.

Experimental description: A single crystal of purple **ferric μ-oxo dimer** was mounted under mineral oil on a Mitegen micromount and immediately placed in a cold nitrogen stream before data collection. The single crystal data was collected on a Bruker Apex DUO equipped with an ApexII CCD detector and a Mo fine-focus sealed source. Data were collected using a combination of phi and omega scans and integrated with the Bruker SAINT program. Structure solution was performed using the SHELXTL software suite. Intensities were corrected for Lorentz and polarization effects and an empirical absorption correction was applied using SADABS v2014/4. Non-hydrogen atoms were refined with

anisotropic thermal parameters and hydrogen atoms were included in riding idealized positions.

A structural model consisting of the host plus approximately seven highly disordered toluene solvate molecules per unit cell was developed; however, positions for the idealized solvate molecules were poorly determined. Since positions for the solvate molecules were poorly determined, a second structural model was refined with contributions from the solvate molecules removed from the diffraction data using the bypass procedure in PLATON. No positions for the host network differed by more than two su's between these two refined models. The electron count from the "squeeze" model converged in good agreement with the number of solvate molecules predicted by the complete refinement. The "squeeze" data are reported here.
The triflate anion is disordered over two orientations. The like S-O, S-C, and C-F distances were restrained to be similar (esd 0.01 Å). Similar displacement amplitudes (esd 0.01) were imposed on disordered sites overlapping by less than the sum of van der Waals radii.

CCDC deposition number: 2515966

Table S2. Crystal data and structure refinement for ferric-μ-oxo dimer.

Identification code	25226_a_sq	
Empirical formula	C44 H60 F6 Fe2 N6 O9 S2	
Formula weight	1106.80	
Temperature	100(2) K	
Wavelength	0.71073 ≈	
Crystal system	Tetragonal	
Space group	$P4_2/n$	
Unit cell dimensions	a = 16.4628(11) ≈	a= 90∞.
	b = 16.4628(11) ≈	b= 90∞.
	c = 22.7913(16) ≈	g = 90∞.
Volume	6177.0(9) $≈^3$	
Z	4	
Density (calculated)	1.190 Mg/m^3	
Absorption coefficient	0.603 mm^{-1}	
F(000)	2304	
Crystal size	0.292 x 0.098 x 0.091 mm^3	

Theta range for data collection	1.964 to 25.384∞.
Index ranges	-19<=h<=19, -19<=k<=19, -27<=l<=27
Reflections collected	89663
Independent reflections	5674 [R(int) = 0.0638]
Completeness to theta = 25.242∞	99.9 %
Absorption correction	Semi-empirical from equivalents
Max. and min. transmission	0.97387 and 0.91205
Refinement method	Full-matrix least-squares on F^2
Data / restraints / parameters	5674 / 199 / 390
Goodness-of-fit on F^2	1.052
Final R indices [I>2sigma(I)]	R1 = 0.0368, wR2 = 0.0966
R indices (all data)	R1 = 0.0511, wR2 = 0.1037
Extinction coefficient	n/a
Largest diff. peak and hole	0.321 and -0.270 e.≈$^{-3}$